Eur Biophys J (2005) 35: 1–26
DOI 10.1007/s00249-005-0001-2

ARTICLE

Andrei L. Kindzelskii · Howard R. Petty

Ion channel clustering enhances weak electric field detection by neutrophils: apparent roles of SKF96365-sensitive cation channels and myeloperoxidase trafficking in cellular responses

Received: 18 January 2005 / Revised: 13 May 2005 / Accepted: 23 June 2005 / Published online: 26 July 2005

Abstract We have tested Galvanovskis and Sandblom's prediction that ion channel clustering enhances weak electric field detection by cells as well as how the elicited signals couple to metabolic alterations. Electric field application was timed to coincide with certain known intracellular chemical oscillators (phase-matched conditions). Polarized, but not spherical, neutrophils labeled with anti-$K_V1.3$, FL-DHP, and anti-TRP1, but not anti-T-type Ca^{2+} channels, displayed clusters at the lamellipodium. Resonance energy transfer experiments showed that these channel pairs were in close proximity. Dose-field sensitivity studies of channel blockers suggested that K^+ and Ca^{2+} channels participate in field detection, as judged by enhanced oscillatory NAD(P)H amplitudes. Further studies suggested that K^+ channel blockers act by reducing the neutrophil's membrane potential. Mibefradil and SKF93635, which block T-type Ca^{2+} channels and SOCs, respectively, affected field detection at appropriate doses. Microfluorometry and high-speed imaging of indo-1-labeled neutrophils was used to examine Ca^{2+} signaling. Electric fields enhanced Ca^{2+} spike amplitude and triggered formation of a second traveling Ca^{2+} wave. Mibefradil blocked Ca^{2+} spikes and waves. Although 10 μM SKF96365 mimicked mibefradil, 7 μM SKF96365 specifically inhibited electric field-induced Ca^{2+} signals, suggesting that one SKF96365-senstive site is influenced by electric fields. Although cells remained morphologically polarized, ion channel clusters at the lamellipodium and electric field sensitivity were inhibited by methyl-β-cyclodextrin. As a result of phase-matched electric field application in the presence of ion channel clusters, myeloperoxidase (MPO) was found to traffic to the cell surface. As MPO participates in high amplitude metabolic oscillations, this suggests a link between the signaling apparatus and metabolic changes. Furthermore, electric field effects could be blocked by MPO inhibition or zremoval while certain electric field effects were mimicked by the addition of MPO to untreated cells. Therefore, channel clustering plays an important role in electric field detection and downstream responses of morphologically polarized neutrophils. In addition to providing new mechanistic insights concerning electric field interactions with cells, our work suggests novel methods to remotely manipulate physiological pathways.

Keywords Electric fields · Calcium signaling · Lipid rafts · Energy transfer · Chemical oscillators

Abbreviations 4-AP: 4-Aminopyridine · di-8-ANEPPS: 1-(3-Sulfonatopropyl)-4-[beta [2-(di-*n*-octylamino)-6-naphtyl]vinyl] pyridinium betaine · ELF: Extremely-low frequency · FcγR: Fcγ receptor · FITC: Fluorescein isothiocyanate · FL-DHP: DM-bodipy (−)-dihydropyridine · FMLP: *N*-formyl-met-leu-phe · HBSS: Hanks' buffered salt solution · pHBAH: *p*-hydroxybenzoic acid hydrazide · HQ: Hydroxyquinone · mβCD: Methyl-β-cyclodextrin · MPO: Myeloperoxidase · OTP: Optical transmembrane potential · PMA: Phorbol myristate acetate · PMT: Photomultiplier tube · RET: Resonance energy transfer · ROM: Reactive oxygen metabolite · SHA: Salicylhydroxamic acid · SOC: Store-operated channel · TEA: Tetraethylammonium chloride · TRITC: Tetramethylisothiocyanate · TRP: Transient receptor potential-like

A. L. Kindzelskii · H. R. Petty (✉)
Department of Ophthalmology and Visual Sciences,
The University of Michigan Medical School,
1000 Wall Street, Ann Arbor, MI, 48105 USA
E-mail: hpetty@umich.edu
Tel.: +1-734-6470384
Fax: +1-734-9363815

H. R. Petty
Department of Microbiology and Immunology,
The University of Michigan Medical School,
Ann Arbor, MI, 48105 USA

Introduction

Under certain conditions, electric fields may interact with cells and tissues (Hoppe et al. 1983). For example,

living organisms use endogenous electric fields to direct cell growth and healing. Electric fields generated during development direct cellular orientation, migration, positioning, and differentiation (Jaffe and Nuccitelli 1977; Nuccitelli 1988; Hotary and Robinson 1994; Shi and Borgens 1995). Therefore, it is not surprising that electric fields direct wound healing at the surface of an organism (Sheridan et al. 1996; Nishimura et al. 1996). Exogenous electric fields also affect cells and tissues. For example, applied electric fields accelerate bone healing in patients (Bassett 1993). Although the mechanism(s) responsible for these effects have not been firmly established, recent studies suggest that extracellular Ca^{2+} and verapamil-sensitive channels participate in exogenous electric field-directed cell growth/extension, migration, and proliferation in DC and AC electric fields at intermediate intensities (Onuma and Hui 1988; Stewart et al. 1995; Zhuang et al. 1997; Lorich et al. 1998; Fang et al. 1998; Cho et al. 1999; Perret et al. 1999; Kenny et al. 1997; Wang et al. 2000). Ca^{2+} channel blockers inhibit galvanotaxis (Trollinger et al. 2002). Furthermore, Ca^{2+} signaling has been linked to electrically-stimulated bone healing (Brighton et al. 2001). Thus, the interaction of intermediate strength electric fields with cells is well established and has demonstrated clinical utility.

Although the interaction of intermediate strength electric fields with cells has become fairly well developed, the interaction of weak extremely low frequency (ELF) electric fields with cells has been controversial. Experimental studies have suggested variously that transmembrane signaling pathways, especially Ca^{2+}, might be involved in cell detection of weak sinusoidal electric fields (Walleczek and Liburdy 1990; Uckum et al. 1995; Yost and Liburdy 1992; Lindstrom et al. 1995; Lyle et al. 1988, 1991). However, these studies have suffered from the lack of a robust experimental observable as well as a rational mechanism linking field exposure to cellular changes. The results, however, are broadly reminiscent of those observed at intermediate field strengths.

One factor left unattended by previous weak electric field studies, which may account for the variability of the findings, is the timing (or phase) of the sinusoidal or pulsed electric field with respect to the endogenous time-dependent chemical oscillators within living cells. For example, neutrophils exhibit oscillations in cell metabolism, intracellular Ca^{2+} release, membrane potential, oxidant production, etc. with periods of ~10 and ~20 s (Petty 2001). Moreover, Gruler and colleagues have shown experimentally and theoretically that intermediate strength pulsed electric fields enhance galvanotaxis of neutrophils when applied with a period of 8 s and that a lag time between field application and response was 8–10 s (Franke and Gruler 1994; Schienbein and Gruler 1995). We have recently reported that when time-varying electric fields are applied to neutrophils during the trough of endogenous NAD(P)H oscillations, the cells greatly extend their length from ~10 μm to ~50 μm, the NAD(P)H oscillation grows dramatically in amplitude, superoxide production is increased, and, as a likely consequence of superoxide production, cellular DNA is damaged (Kindzelskii and Petty 2000; Rosenspire et al. 2000, 2001). In contrast, if weak time-varying electric fields are applied to cells at some other point in their chemical oscillatory cycle, the effects disappear and the cells become spherical in shape. Thus, the exogenous electric field's phase relative to intracellular chemical oscillators is a key parameter in gathering robust data.

Although our prior studies have outlined the metabolic and chemical events leading to DNA damage due to weak extremely-low frequency (ELF) electric fields, we have not identified the early transmembrane signaling events contributing to these changes. We hypothesized that elements of the Ca^{2+} signaling apparatus participate in cellular responses to appropriately phase-aligned electric fields. Several observations supported the formulation of this hypothesis. First, as described above, intermediate strength electric fields appear to utilize Ca^{2+} signaling pathways. Second, the ability of phase-matched DC and AC electric fields to increase metabolic oscillation amplitudes is shared with interferon-γ, interleukin-12, and PMA (a tumor promoter), which all signal via Ca^{2+} pathways (Aas et al. 1998, 1999; Petty 1993; H.R. Petty, unpublished) to enhance oscillatory metabolic amplitudes and oxidant production (Adachi et al. 1999; Berton et al. 1986; Ding et al. 1988). Third, theoretical studies have suggested that weak ELF fields may interact with the intracellular Ca^{2+} oscillator (Eichwald and Kaiser 1993, 1995; Galvanovskis and Sandblom 1997).

The theoretical study of Galvanovskis and Sandblom (1997) is particularly interesting as they suggest several conditions that might promote weak electric field detection by cells, some of which are directly accessible to experimental examination. One prediction of Galvanovskis and Sandblom (1997) is that ion channel clustering promotes the detection of weak electric fields. The present study confirms this prediction by showing: (1) morphologically polarized neutrophils exhibit $K_v1.3$ and Ca^{2+} channel clusters at the lamellipodium and are responsive to weak electric fields whereas spherical cells display more uniformly distributed channels and are not responsive to these fields. (2) Channel blockers whose targets include channels known to cluster inhibit the effects of electric fields. (3) SKF96365-sensitive channels are the earliest step associated with electric field-specific Ca^{2+} spikes and waves. (4) As these channels are associated with lipid rafts, mβCD, which has been reported to disrupt lipid rafts, blocks channel cluster formation and, in parallel, inhibits electric field-induced effects. Our work suggests that membrane channels, channel clustering and the Ca^{2+} signaling apparatus participate in mediating cellular responses to weak electric fields, provided that the membrane potential is intact. We went on to show that these signals apparently promote the trafficking of myeloperoxidase to the cell surface, thereby promoting the peroxidase cycle, which enhances the amplitude of metabolic oscillations. In addition to providing dramatic evidence in support of the Galva-

novskis and Sandblom model, we have defined experimentally several additional parameters that may be used to refine this model. Furthermore, a broad-based biological model of weak electric field-cell interaction is proposed.

Materials and methods

Materials

TRITC, FITC, indo-1-AM, FL-DHP (DM-bodipy (−)-dihydropyridine), di-8-ANEPPS, and Pluronic F-127 (20% solution in DMSO) were obtained from Molecular Probes, Inc. (Eugene, OR, USA). Tetraethylammonium chloride (TEA), 4-aminopyridine (4-AP), mibefradil, verapamil, nifedipine, SKF96365, and methyl-β-cyclodextrin (mβCD), were purchased from Sigma Chemical Co. (St. Louis, MO, USA). The myeloperoxidase (MPO) inhibitors salicylhydroxamic acid (SHA), *p*-hydroxybenzoic acid hydrazide (pHBAH), cyanide, and hydroxyquinone (HQ) were purchased from Sigma. Native MPO was also purchased from Sigma.

Cells

Neutrophils were isolated from the peripheral blood of normal healthy adults using Ficoll-Hypaque (Sigma) density gradient centrifugation (Sehgal et al. 1993). Purified cells were >95% viable as judged by trypan blue exclusion.

Anti-Kv1.3, anti-TRP-1 and anti-MPO antibodies

Polyclonal rabbit anti-Kv1.3, anti-TRP1 and anti-lactate dehydrogenase antibodies were purchased from Chemicon International Inc. (Temecula, CA, USA). Both of these antibodies were prepared using human peptides. Anti-FcγRIII (Medarex, Princeton, NJ, USA) was used as a negative control. A FITC-conjugated anti-human MPO antibody was purchased from Accurate Chem. Inc. (Westbury, NY, USA).

For TRITC antibody conjugation, the pH of antibody solution was increased by overnight dialysis against carbonate buffer (pH 9.6; 0.2 M). TRITC was then added at a molar ratio 1:13 for 3 h with shaking followed by overnight dialysis against PBS (pH 7.4) and Sephadex G25 column chromatography.

Anti-T-type Ca^{2+} channel antibody

Several previous workers have prepared polyclonal antibodies directed against the T-type Ca^{2+} channel (Andreasen et al. 2000; Weiergraber et al. 2000). The antibody was prepared as described by Andreasen et al. (2000) by using a peptide corresponding to amino acids 1 to 22 of the NH_2 terminal region of human α1G subunit of the low voltage T-type Ca^{2+} channel (NCBI locus AF126966) with addition of a C-terminal cysteine: NH_2-MDEEEDGAGAEESGQPRSFMRL(C)-COOH.

The purified peptide was conjugated to KLH then used to immunize rabbits (Bio-Synthesis Inc., Lewisville, TX, USA). The IgG fraction was found to specifically label cells.

mβCD treatment of cells

Lipid rafts have been reported to be disrupted by mβCD treatment. Neutrophils were incubated in buffer containing 5 mM mβCD for 5 min at 37°C as described (Sitrin et al. 2004).

Electrode configuration

Electric fields were applied as described (Kindzelskii and Petty 2000; Petty 2000; Rosenspire et al. 2000, 2001). Briefly, chambers were constructed using two parallel Pt electrodes (0.25 mm in diameter) separated by 11 mm. Electrodes were attached to a glass microscope slide. A coverslip was placed over the electrodes; the apparatus was sealed with silicone grease. This gave the chamber dimensions of 0.254 mm×11 mm×25.4 mm. The resistivity of the medium was typically 140 *Ohm* cm. In some experiments samples were isolated from the electrodes using a gelatin matrix. A power supply was used to apply pulsed square wave DC electric fields of various intensities. The pulsed field was applied manually during observations. Electric field intensities were determined by measuring the current using an electrometer (Keithley, Cleveland, OH, USA; model 6517A), which has an extremely low voltage burden, fast settling time and high resolution.

Indirect immunofluorescence staining

Fluorescence microscopy was performed with an Axiovert 135 fluorescence microscope with a high numerical aperture condenser, quartz objective, and an AttoArc mercury lamp (Zeiss). Cells attached to coverslips were fixed with 3.7% paraformaldehyde for 30 min at room temperature then blocked with 3% BSA then immunostained. For double-staining experiments, fixed cells were washed several times with HBSS then labeled with TRITC-conjugated polyclonal rabbit antibody against K_v1.3 channel (10 μg/ml) for 1 h at room temperature. After several washes cells were fixed again with 3.7% paraformaldehyde and blocked with 3% BSA in HBSS, followed by labeling with FITC-conjugated anti-TRP1, anti-T-type channel, anti-CD16 or FL-DHP for 1 h at room temperature. After extensive washing the coverslip was inverted and mounted on a slide. The stained cells were observed using conventional fluorescence

microscopy. In other cases, images from multiple focal planes were collected using a z-scan apparatus (Veytek, Inc., IA, USA) and a cooled Retiga 1300 camera (Q-Imaging, BC, Canada) or an intensified charge-coupled device camera (Hamamatsu, Hamamatsu City, Japan). Images were managed, processed and deconvoluted using Supermicro Ultra 320 workstation with the software packages: Image-Pro, Microtome, Image-Scan, and Vox-Blast (Veytek, Inc.). In both cases, narrow bandpass filters were used to obtain specific fluorescence. Representative sections of immunostained fluorescent samples are shown below.

Optical transmembrane potential labeling

Di-8-ANEPPS was added to adherent neutrophils at a final concentration of 5 μM. Pluronic F-127 (0.05%) was used to enhance labeling. Cells were incubated with dye at 4°C for 30 min followed by extensive washing.

Microfluorometry

Quantitative microfluorometry and excitation spectroscopy were performed on single cells using a Peltier-cooled photomultiplier tube (PMT) D104 system (Photon Technology Int., Lawrenceville, NJ, USA) attached to a Zeiss axiovert 35 (Carl Zeiss, Inc., New York, NY, USA) fluorescence microscope. A monochromator and a fiber-optically coupled xenon lamp were controlled by FeliX software (Photon Tech.). Cells were labeled with indo-1-AM at 5 μg/ml for 20 min at 37°C, as described (Sehgal et al. 1993; Kindzelskii and Petty 2003). During microfluorometry of indo-1-labeled cells the excitation and emission wavelengths were set using excitation at 350 nm (10 nm band-pass) and emission was detected using a 400LP dichroic mirror and a 405DF43 emission filter. For short time base experiments (e.g., 500 data points/s), it was necessary to both increase the illumination light level and to increase the gain of the amplifier. The probe di-8-ANEPPS was used with excitation and emission wavelengths of 465 nm and 610 nm (610/22 DF), respectively. For this probe a long-pass dichroic mirror at 560 nm (Omega Optical) was employed. The PMT output was recorded as a function of time.

High-speed imaging and emission spectroscopy

High-speed imaging was performed using an axiovert 135 fluorescence microscope with a quartz condenser, quartz objective, and an AttoArc mercury lamp (Zeiss). To image the low wavelength indo-1 region, a 355HT15 exciter, 390LP dichroic reflector and a 405DF43 emission filter were employed. To increase light collection efficiency, the microscope's bottom port was employed. This port was fiber-optically coupled to the input of an Acton-150 (Acton Instruments, Acton, MA, USA) imaging spectrophotometer. The exit side was connected to a liquid N_2-cooled intensifier attached to a Peltier-cooled I-MAX-512 camera (~−20°C) (Princeton Instruments Inc., Trenton, NJ, USA) (Petty and Kindzelskii 2000; Petty et al. 2000; Kindzelskii and Petty 2003, 2002). A Gen-II tube was used to provide maximal efficiency in the violet-blue region of the spectrum. The camera was controlled by a high-speed Princeton ST-133 interface and a Stanford Res. Systems (Sunnyvale, CA, USA) DG-535 delay gate generator (Petty et al. 2000). A custom-built computer with dual 3.06 GHz Xenon processors with 1 MB onboard cache each, 3.0-Gb RAM, 3.2 Tb of hard drive space with 64MB cache, and a RAID-5 hard drive management system was used. For experiments, 2 Gb of RAM was allocated as a RAM disk. Winspec-32 (version 2.5.14.1; Princeton Instruments) software was used with a PCI communication accelerator. To improve computer acquisition times, the size of the pixel detection array of the CCD chip was adjusted using a Virtual-Chip plug-in. Winspec CPU calls were given system priority to enhance the instrument's duty cycle. Data were acquired without reporting to the monitor to further improve system speed.

Reproducibility of results

In the experiments listed below, the number of independent days upon which the results were replicated are given as n. For conventional imaging experiments, roughly 50–100 cells were examined each day. Fewer cells, approximately 10 per day, were studied with high speed and z-scan deconvolution microscopy.

Results

Although previous studies from this laboratory have demonstrated that neutrophils are capable of detecting pulsed weak (10^{-4} V/m) electric fields (Kindzelskii and Petty 2000; Rosenspire et al. 2001) as well as applied magnetic fields (Rosenspire et al. 2003), the early mechanistic steps in field detection are unknown. The present study tests the hypothesis that membrane channels and Ca^{2+} signaling participate in this process.

$K_v1.3$ Channels, FL-DHP Binding Sites, and TRP1 Cation Channels, but not T-type Ca^{2+} Channels, Cluster at the Lamellipodium of Polarized Neutrophils

Galvanovskis and Sandblow's (1997) theory predicts that weak electric field detection is enhanced on cells with clustered ion channels. To test this possibility we studied K^+ and Ca^{2+} channels of human neutrophils. These channels are known to participate in signaling for ROM production by neutrophils, which is one consequence of neutrophil exposure to weak phase-matched electric fields (Kindzelskii and Petty 2000). Localization

of K^+ channel $K_v1.3$ was performed by indirect immunofluorescence. The experiment in Fig. 1a, b shows cells treated with an electric field, fixed, then labeled with a monospecific anti-$K_v1.3$ Ab. As previously noted (Kindzelskii and Petty 2000), the orientation of the applied field relative to the direction of morphological polarization of the cell apparently has no effect on field sensitivity. As this figure shows, the cell phase-matched with the field elongated and demonstrated bright labeling of $K_v1.3$ at the lamellipodium. In contrast, the spherical cell in this same experiment did not respond to the electric field with a shape change and exhibited a uniform membrane distribution of $K_v1.3$. The cell surface features of Ca^{2+} channels were also studied. Neutrophils (Fig. 1c, d) were labeled with 50 μg/ml (30 min at 19°C) fluorescent dihydropyridine FL-DHP then washed as described (Knaus et al. 1992a, 1992b; Berger et al. 1994). This molecule has been reported to bind to L-type Ca^{2+} channels, (Shaw and Quatrano 1990; Goligorsky et al. 1995; Nachman-Clewner et al. 1999; Schild et al. 1995; Oshima et al. 1996; Vallee et al. 1997; Knaus et al. 1992a, b; Berger et al. 1994), although DHPs may bind to other classes of Ca^{2+} channels as well (Willmott et al. 1996; Sadighi et al. 1996). Although non-adherent cells were uniformly labeled with FL-DHP, polarized cells were predominantly labeled at the lamellipodium (Fig. 1d). Thus, cells exposed to an electric field, rapidly fixed as described (Kindzelskii and Petty 2000), then labeled with FL-DHP, showed intense and localized labeling of the lamellipodium (Fig. 1d). However, cells labeled with anti-T-type Ca^{2+} channel antibody did not show such a dramatic redistribution to the lamellipodium (Fig. 1e, f). Inasmuch as the TRP proteins represent a novel, important class of membrane cation channels, including those with store-operated properties, we also analyzed the cell surface distribution of TRP1. Figure 1g, h shows that anti-TRP1 antibodies brightly label the lamellipodium of polarized neutrophils, suggesting a redistribution of these channels as well. Hence, TRP-1, $K_v1.3$, and HL-DHP binding sites, but not T-type channels, demonstrate enhanced labeling of the lamellipodium.

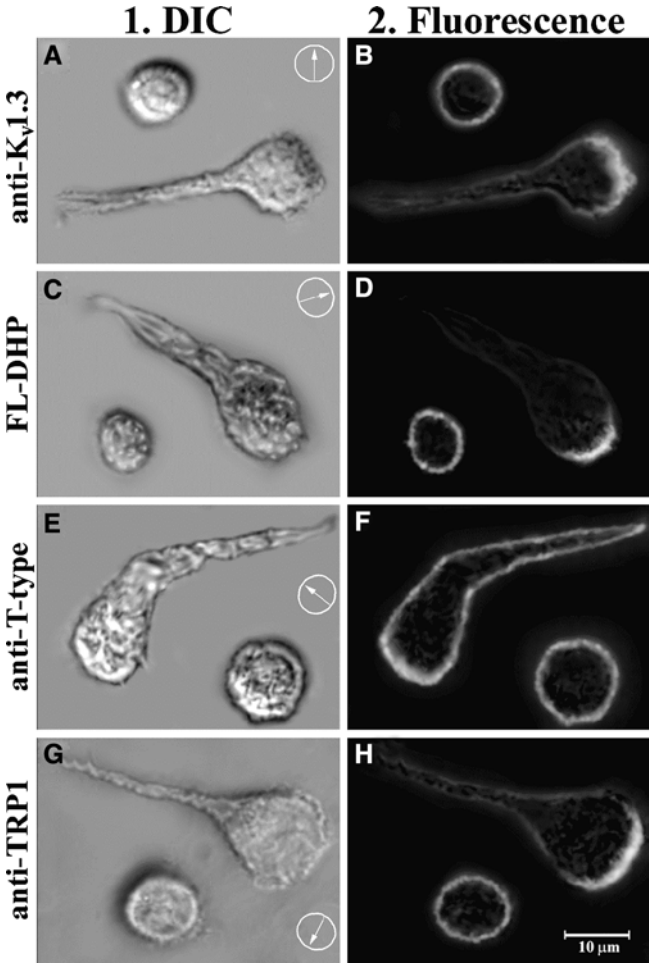

Fig. 1 The distribution of membrane channels on morphologically polarized neutrophils. DIC (**a**, **c**, **e**, and **g**) and fluorescence (**b**, **d**, **f**, and **h**) micrographs are shown. The micrographs were chosen to illustrate that facts that morphologically polarized neutrophils exposed to electric fields (0.4 V/m, 200 ms) phase-matched to intracellular chemical oscillators extend their lengths (**a**, **c**, **e** and **g**) and express clusters of certain ion channels at the lamellipodium (**b**, **d** and **h**). The spherical cells in each experiment serve as internal controls. After exposure to a phase-matched field for about 8 min (roughly 28 pulses), samples were fixed with 3.7% paraformaldehyde then stained with anti-$K_v1.3$ (**a**, **b**), FL-DHP (**c**, **d**), anti-T-type Ca^{2+} channel (**e**, **f**), and anti-TRP1 (**g**, **h**). $K_v1.3$, TRP1, and FL-DHP binding sites are predominantly found at the leading edge of the cells, whereas the distribution of T-type channels is more uniform. The polarity of the electric field is indicated on the DIC micrographs in this and subsequent figures by a *circled arrow*. Each of the experiments was repeated on six different days ($n = 6$) with indistinguishable results. The channel distributions of ≥30 cells phase-matched to an applied electric field were studied on each day. (×1,180) (*bar* = 10 μm)

Although Fig. 1 suggests that ion channels are clustered following exposure to a phase-matched electric field, it does not reveal if $K_v1.3$ and TRP1 channels were clustered prior to field application. As ion channel clustering is a proposed requirement for field detection (Galvanovskis and Sandblom 1997), we examined cells in the absence of applied fields. Morphologically polarized cells were examined in the absence of electric field exposure. These cells also displayed enhanced membrane channel labeling of the lamellipodium. This was observed for the same reagents noted above (Kv1.3, FL-DHP, and TRP1), as illustrated in Fig. 2. The asymmetric distributions of $K_v1.3$, TRP1 and FL-DHP binding sites and the accompanying sensitivity of morphologically polarized cells to weak electric fields are consistent with theoretical predictions and support the hypothesis that channel clustering enhances electric field sensitivity (Galvanovskis and Sandblom 1997).

Although Figs. 1 and 2 strongly support extensive channel redistribution, we have provided additional support using z-scan optical imaging followed by deconvolution analysis. This method corrects for the potential contribution of out-of-focus fluorescence to the apparent fluorescence intensity of the lamellipodium. Figure 3 shows representative deconvoluted images of

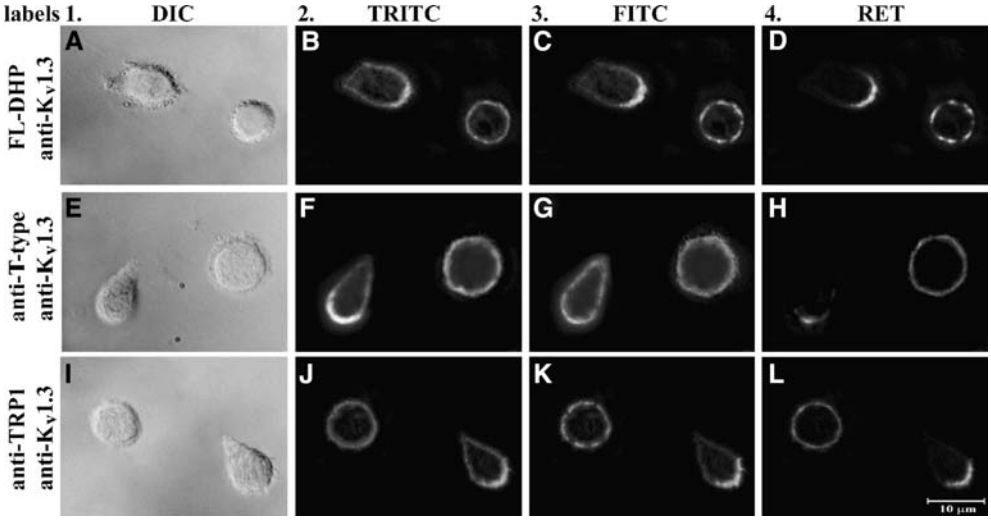

Fig. 2 Fluorescence microscopic detection of membrane channel co-localization and resonance energy transfer. *Column 1* shows DIC micrographs of cells (**a**, **e**, **i**). *Columns 2* and *3* show fluorescence micrographs of cells imaged with TRITC (**b**, **f**, **j**) and FITC (**c**, **g**, **k**) optical filters. TRITC images were collected using emission and excitation filters at 540/20 nm and 590/30 nm and a dichroic mirror at 510 nm. FITC images were collected using emission and excitation filters at 485/22 nm and 530/30 nm and a dichroic mirror at 560 nm. On the right hand side, *column 4* (**d**, **h**, **l**) shows the fluorescence RET emission. RET studies were performed using an excitation filter of 485/22 nm, an emission filter of 590/30 nm and a dichroic mirror at 510 nm. In contrast to the cells of Fig. 1, these cells were not exposed to an electric field. In all experiments neutrophils were labeled with TRITC-anti-K_v1.3 antibodies. Neutrophils were also labeled with: FL-DHP in panels **a**–**d**, FITC-anti-T-type channel in panels **e**–**h**, and FITC-anti-TRP1 channel in panels **i**–**l**. Although RET was pronounced at the lamellipodium of polarized cells, a lower level of RET was found associated with spherical cells. Spectroscopic controls using cells labeled with only TRITC or FITC showed that cross-talk between the filter sets was not significant at the gain settings used. These findings and interpretations are further supported by the emission spectroscopy studies shown in Fig. 4. Thus, certain channels cluster at the lamellipodium of polarized neutrophils in the presence (Fig. 1) or absence (this figure) of an applied electric field. Furthermore, these channels are in close proximity to one another as judged by RET. ($n = 5$) (×1,190) (*bar* = 10 μm)

K_v1.3 and TRP1. It was not possible to perform z-scan analyses on FL-DHP due to its weak intensity and photobleaching. As suggested by Figs. 1 and 2, Kv1.3 and TRP1 can be found about the spherical cells (Fig. 3a, b, e, f). These findings suggest that Kv1.3 and TRP1 may be found within clusters in the plasma membrane. When cells were examined during exposure to phase-matched electric fields, both Kv1.3 and TRP1 were found to cluster (Fig. 3d,h). Therefore, the formation of large ion channel-rich domains can be observed.

Physical proximity of K_v1.3 K^+ channels and Ca^{2+} channel labels

The co-localization of K_v1.3 and Ca^{2+} channels at the lamelliopodium suggest that they may be adjacent to one another in the membrane. To assess the physical proximity of K_v1.3 and Ca^{2+} channels on neutrophils, RET experiments were conducted on cells labeled with donor and acceptor-labeled reagents. Cells were labeled with FL-DHP and rhodamine-conjugated anti-K_v1.3, as described above. Figure 2a–c shows the distribution of FL-DHP and anti-K_v1.3 on cells, which recapitulate the findings noted above. The labeling patterns of FL-DHP and anti-K_v1.3 differ on both spherical and polarized cells. For example, FL-DHP appears to be excluded from the body of polarized cells and its labeling pattern on spherical cells is much more punctate than that of K_v1.3 (Fig. 2b vs. c). Thus, FL-DHF and anti-K_v1.3 labeling are not identical, which suggests that FL-DHP is not binding to Kv channels in these experiments. Using well-established methods in this laboratory (e.g., Kindzelskii et al. 1996 1997, 2000; Zarewych et al. 1996; Sitrin et al. 2001), we have observed RET between these two membrane channels on neutrophils. Figure 2d shows that RET emission is most intense in a region of the lamellipodium, although intensity is also found in clumps about the periphery of the spherical cell. We next performed RET experiments using the Ab labels for the T-type Ca^{2+} channel and the TRP1 cation channel. The T-type Ca^{2+} channel was primarily found in a uniform distribution about the perimeter of both spherical and polarized cells (Fig. 2g). RET between K_v1.3 and T-type Ca^{2+} channels was detected (Fig. 2h), although its intensity was below that of FL-DHP and anti-TRP1-labeled cells. Anti-TRP1 staining resembled that of FL-DHP (Fig. 2k,c, respectively). Furthermore, RET was detected between K_v1.3 and TRP1 (Fig. 2l). In contrast to these results, cells stained with anti-K_v1.3 and anti-CD16 did not display RET, which constitutes a negative control. Therefore, as anticipated, RET is not a general property of membrane proteins. Furthermore, RET was found to be especially strong on polarized cells.

These RET imaging results were confirmed using fluorescence spectrophotometry of individual cells using an imaging spectrophotometer. The fluorescence emission spectra of FITC and TRITC labels are shown in

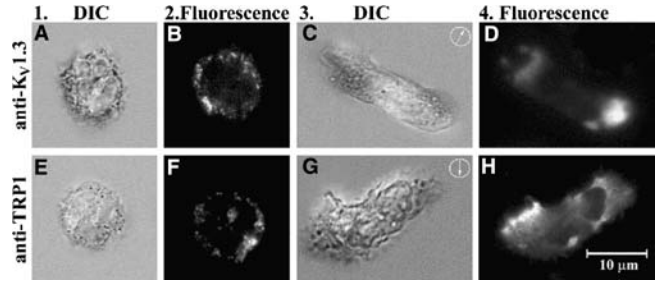

Fig. 3 The distribution of neutrophil membrane channels revealed by z-scan deconvolution analyses. DIC (**a**, **c**, **e**, **g**) and fluorescence (**b**, **d**, **f**, **h**) micrographs are shown. Cells were not exposed to electric fields (**a**, **b**, **e**, **f**) or exposed to phase-matched electric fields (0.4 V/m, 200 ms, approximately 15 pulses) (**c**, **d**, **g**, **h**). Cells were fixed then labeled with TRITC-anti-K_v1.3 antibodies (**a**–**d**) or FITC-anti-TRP1 antibodies (**e**–**h**). Although clusters of channels are found under all conditions, large clusters of channels can be found at the lamellipodia of neutrophils exposed to phase-matched electric fields. ($n = 3$) (×450) (*bar* = 10 μm)

Fig. 4a. In this case cells were only labeled with the donor or the acceptor molecules. In Fig. 4b we show the presence of the rhodamine emission peak at approximately 580 nm during excitation of FL-DHP, thus indicating RET between these two labels. Further studies using the anti-K_v1.3 reagent with anti-T-type channel (Fig. 4c) and anti-TRP1 (Fig. 4d) also demonstrated RET. However, spectrophotometry studies of anti-K_v1.3 and anti-CD16 did not exhibit RET. The data of Figs. 2 and 4 clearly indicate that these channels are in close physical proximity (< 7 nm) on cells. Therefore, certain K^+ and Ca^{2+} channels are likely nearest neighbors on cells.

Fig. 4 Emission microspectrophotometry of resonance energy transfer between membrane channels. The wavelength (nm) is shown at the abscissa whereas the emission intensity (counts/s) is given at the ordinate. **a** Cells were labeled with only FITC-anti-T-type channel or only TRITC-anti-K_v1.3 antibodies after fixation. Excitation for FITC was provided by a 485/22 nm band-pass filter whereas TRITC excitation was provided by a 540/20 nm band-pass filter. Neutrophils were labeled with TRITC-anti-K_v1.3 and FL-DHP in (**b**), TRITC-anti-K_v1.3 and FITC-anti-T-type Ca^{2+} channel in (**c**), and TRITC-anti-K_v1.3 and FITC-anti-TRP1 antibody in (**d**). Negative control experiments were performed by staining cells with TRITC-anti-K_v1.3 and FITC-anti-CD16 reagents, which did not display detectable RET in (**e**). RET can be observed among certain membrane proteins using emission spectroscopy

Effect of K^+ and Ca^{2+} channel blockers on metabolic resonance

If membrane channel clusters participate in the detection of weak electric fields, channel blockers should influence cell responses to these fields. Therefore, we examined the effect of verapamil on the ability of phase-matched pulsed DC fields to trigger metabolic resonance. As we have reported previously (Petty 2000; Kindzelskii and Petty 2000; Rosenspire et al. 2000), the application of frequency- and phase-matched electric fields causes metabolic resonance in neutrophils (Fig. 5e vs. a). A verapamil dose of 110 μg/ml (30 min at 37°C) was found to inhibit metabolic resonance (Fig. 5f), although it had no immediate effect on untreated cells (Fig. 5b). Our studies indicated that the effect of verapamil was both time- and concentration-dependent. The time of 30 min was chosen because it was an easily accessible experimental incubation time and it was effective over a range of doses. A pulsed (200 ms duration) DC electric field of 0.4 V/m was used, although the effects can be observed at field intensities as low as 10^{-4} V/m (Kindzelskii and Petty 2000; Rosenspire et al. 2000, 2001; see below). The intensity of 0.4 V/m was chosen because it is far above the minimal field intensity required for metabolic resonance and therefore the disappearance of metabolic resonance could not be explained by the use of a borderline field intensity, i.e., we wanted to show clearly that the effect was blocked. Although phase-matched electric fields increase the amplitude of metabolic oscillations in neutrophils, application of this same field to verapamil-treated cells has no effect (Fig. 5f). Therefore, the high amplitude NAD(P)H oscillations seen during exposure to weak electric fields are inhibited by verapamil.

We next sought to ascertain the dose–response characteristics of verapamil on the electric field sensitivity of neutrophils. Figure 6a shows the verapamil dose-electric field cut-off response curve. The electric field cut-off is defined as the minimum field intensity that supports metabolic resonance (Kindzelskii and Petty 2000). As shown, electric field sensitivity is affected by verapamil. The verapamil data exhibit a 50% reduction in field sensitivity at about 75 μg/ml. This concentration of verapmil is in agreement with the doses previously reported to block K^+ channels (Robe and Grissmer 2000; Rauer and Grissmer 1999).

In as much as verapamil can interact with K^+ channels as well as Ca^{2+} channels, we examined the potential role of K^+ channels in electric field-mediated

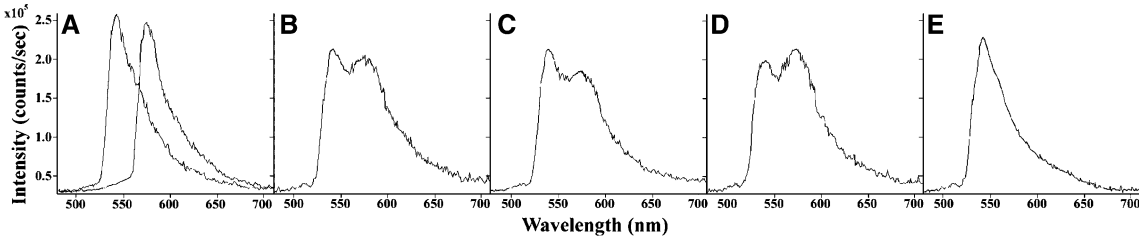

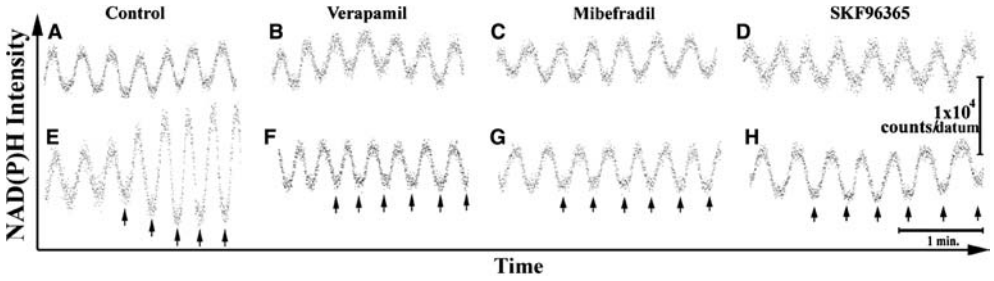

Fig. 5 The effect of electric field application on the properties of metabolic oscillations. The NAD(P)H autofluorescence intensity (ordinate) in counts is plotted vs. time (abscissa) at 20 data points/s The *upper row* shows cells before whereas the *lower row* show cells during electric field exposure. A brief DC electric field (0.4 V/m, 200 ms) was applied at the arrowheads given in the lower row. Control cells show that electric fields application during the trough of the NAD(P)H oscillation leads to the formation of high amplitude oscillations, as previously described (Kindzelskii and Petty 2000), a phenomenon we refer to as metabolic resonance. We have found that certain channel blockers inhibit metabolic resonance. Verapamil at 100 μg/ml blocks metabolic resonance within 30 min (*column 2*). Mibefradil, an inhibitor of T-type Ca^{2+} channels, inhibits metabolic resonance at a dose of 5 μM (*column 3*). In addition, SKF96365, an inhibitor of SOCs, blocks metabolic resonance at a concentration of 4 μM (*column 4*). Thus, at appropriate doses, these channel blockers interfere with cellular responses to phase-matched DC electric field application. *Vertical bar* = 10^4 counts/s. *Horizontal bar* = 1 min

metabolic resonance. To test the role of K^+ channels in metabolic resonance, cells were treated with K^+ channel blockers. Neutrophils were separately treated with the well-known K^+ channel blockers TEA and 4-AP. Dose-response studies (Fig. 6b, c) showed that 1.5 mM TEA or 11μM 4-AP block metabolic resonance during phase-matched electric field exposure. These doses are consistent with the concentrations expected for K^+ channels in leukocytes (e.g., Lin et al. 1993; Lewis and Cahalan 1995; Blunck et al. 2001). The slopes of the dose–response curves are high, which may be accounted for by the fact that this late physiological output is dependent upon the ignition of chemical waves (see below) and is measured in single cells. However, in these cases kinetic experiments revealed that roughly 20–25 min were required to block the acquisition of high amplitude metabolic oscillations (data not shown). As the time required for the inhibitors to bind to K^+ channels is much less than the time required by K^+ channels to exhibit a bioeffect, they are not likely to be the initial field detector.

We next evaluated the effect of Ca^{2+} channel blockers on cellular detection of weak electric fields. The reagent nifedipine, a more specific Ca^{2+} channel blocker than verapamil, was employed. Although nifedipine may affect metabolic resonance (Fig. 6d), the inhibitory concentration (~1 mM) is several orders of magnitude greater than its K_d for L-type Ca^{2+} channels (~1 nM). Therefore, the effect of nifedipine is likely to be non-specific in nature; it can be considered as a good negative control. We next tested the potential role of T-type low voltage-gated Ca^{2+} channels. The reagent mibefradil is known to block T-type Ca^{2+} channels (Perez-Reyes 2003). Figure 6e shows the mibefradil dose-electric field cut-off response curve. As these data show, mibefradil inhibits electric field intensity by 50% at about 1 μM. This concentration of mibefradil is in agreement with the doses needed to effect neutrophil activation and it is consistent with binding to T-type channels (Perez-Reyes 2003). Furthermore, the incubation time with mibefradil needed to block metabolic resonance was brief (< 5 min), suggesting that T-type Ca^{2+} channels participate in cell sensitivity to electric fields prior to K^+ channels.

As SOCs have been found to be a crucial element of the Ca^{2+} signaling apparatus (Itagaki et al. 2002), we have also tested the effect of SKF96365, which inhibits SOCs and certain TRP family proteins (Pizzo et al. 2001; Halawszovich et al. 2000). SKF96365 was found to inhibit metabolic resonance at 3.5 μM for 4 min at 37°C (Fig. 5h). Half-maximal inhibition with SKF96365 occurred at about 9 μM (Fig. 6f), which is consistent with the literature (Halaszovich et al. 2000; Hayat et al. 2003). Electric field sensitivity was also rapidly inhibited by SKF96365, suggesting that it is acting at a relatively early point in electric field stimulation.

Detection of the optical transmembrane potential

Our findings suggest that both K^+ and Ca^{2+} channels participate in sensing weak electric fields. This raises the mechanistic issue of how at least three different channels could be important in field detection. However, a solution is suggested by the facts that: (1) the T-type Ca^{2+} channel is only functional within a range of membrane potentials (Perez-Reyes 2003) and (2) the K^+ channel $K_v1.3$ is the K^+ leak channel of leukocytes (Leonard et al. 1992; Koo et al. 1997) and therefore sets the magnitude of the membrane potential. This immediately suggests that verapamil, TEA, and 4-AP may act by inhibiting the K^+ leak current and, thereby, the membrane potential. We therefore tested the ability of verapamil, TEA, and 4-AP to affect membrane potential. Changes in the transmembrane potential were monitored using the fluorescent dye di-8-ANEPPS, which has an emission intensity proportional to the magnitude of the membrane potential (Witkowski et al. 1998). The fluorescence intensity measured is then interpreted as the optical transmembrane potential (OTP). Previous studies have shown that morphologically polarized neutrophils

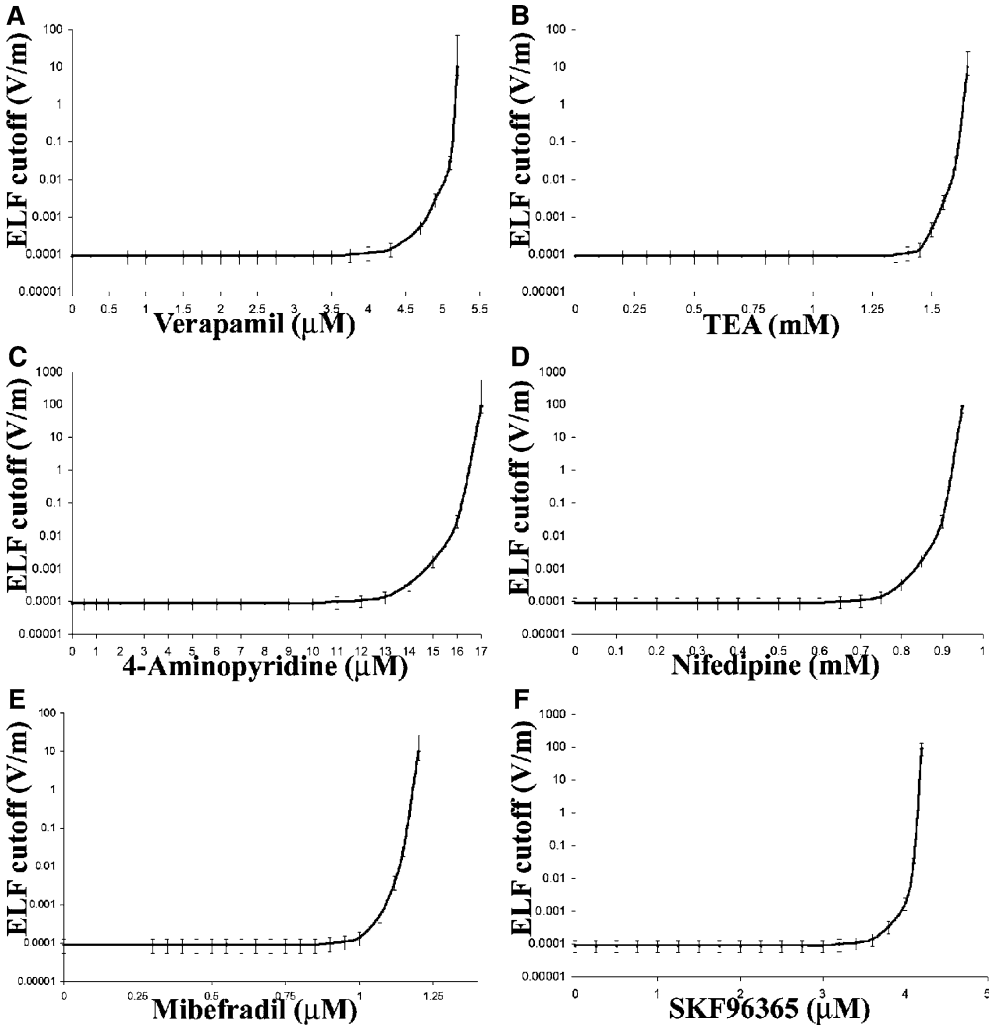

Fig. 6 Dose-response analysis of electric field sensitivity in the presence of membrane channel blockers. The minimum electric field intensity (ELF cut-off) necessary to induce metabolic resonance is plotted vs. the concentration of verapamil (**a**), TEA (**b**), 4-AP (**c**), nifedipine (**d**), mibefradil (**e**) and SKF96365 (**f**). The 50% inhibition concentrations were found to be 4.65 ± 0.12 μM for verapamil, 1.49 ± 0.06 mM for TEA, 13.85 ± 0.35 μM for 4-AP, 0.79 ± 0.05 mM for nifedipine, 1.06 ± 0.06 μM for mibefradil, and 3.78 ± 0.11 μM SKF96365. Incubations were performed for 15 min at room temperature, except for verapamil, which was performed for 30 min. As the concentration of inhibitor is increased, cells become less sensitive to electric fields. Verapamil inhibits metabolic resonance at a concentration consistent with binding to potassium channels. The potassium channel blockers EA and 4-AP are active at concentrations expected for potassium channel inhibition (**b**, **c**). However, the concentration of nifedipine required to block metabolic resonance is much too high to be accounted for by its ability to block L-type Ca^{2+} channels (**d**). Mibefradil and SKF96365, T-type Ca^{2+} channel and SOC blockers, respectively, inhibit metabolic resonance at concentrations consistent with specific channel blockage (**e**, **f**). Thus, cellular detection of electric fields is sensitive to certain types of channel blockers

exhibit an oscillatory membrane potential (Jager et al. 1988). Figure 7a, trace 1 confirms this prior observation using different methodology. To establish that these oscillations in fluorescence intensity were an indication of membrane potential, the OTP of neutrophils was measured in a flow-through microscope chamber (Albrecht and Petty 1998) in the absence and presence of a high K^+ solution. Buffers containing high K^+ concentrations are known to disrupt normal transmembrane potentials of neutrophils (Luscinskas et al. 1988). When a high sodium buffer is replaced with an iso-osmotic high K^+ buffer using rapid injection into the flow-through chamber, the OTP oscillations rapidly disappear (Fig. 7a, trace 2). However, when the high K^+ buffer was replaced with the original buffer, the oscillatory OTP returned (Fig. 7a, trace 2).

Previously described oscillations of neutrophils, such as Ca^{2+} and NAD(P)H oscillations, have taken the form of spikes and sine waves. In contrast, these OTP traces are in the form of sawtooth waves (Fig. 7a, trace 1). Thus, the OTP of morphologically polarized neutrophils is characterized by slow rise followed by a rapid depolarization. We hypothesize that the slow rise in OTP is due to the membrane Na^+/K^+-ATPase, which is electrogenic and a primary contributor to charge displacement across a cell membrane (Majander and Wikstrom 1989). To test this concept, we examined the OTP at several concentrations of ouabain, an inhibitor of the Na^+/K^+-ATPase. Figure 7a, trace 3 illustrates the

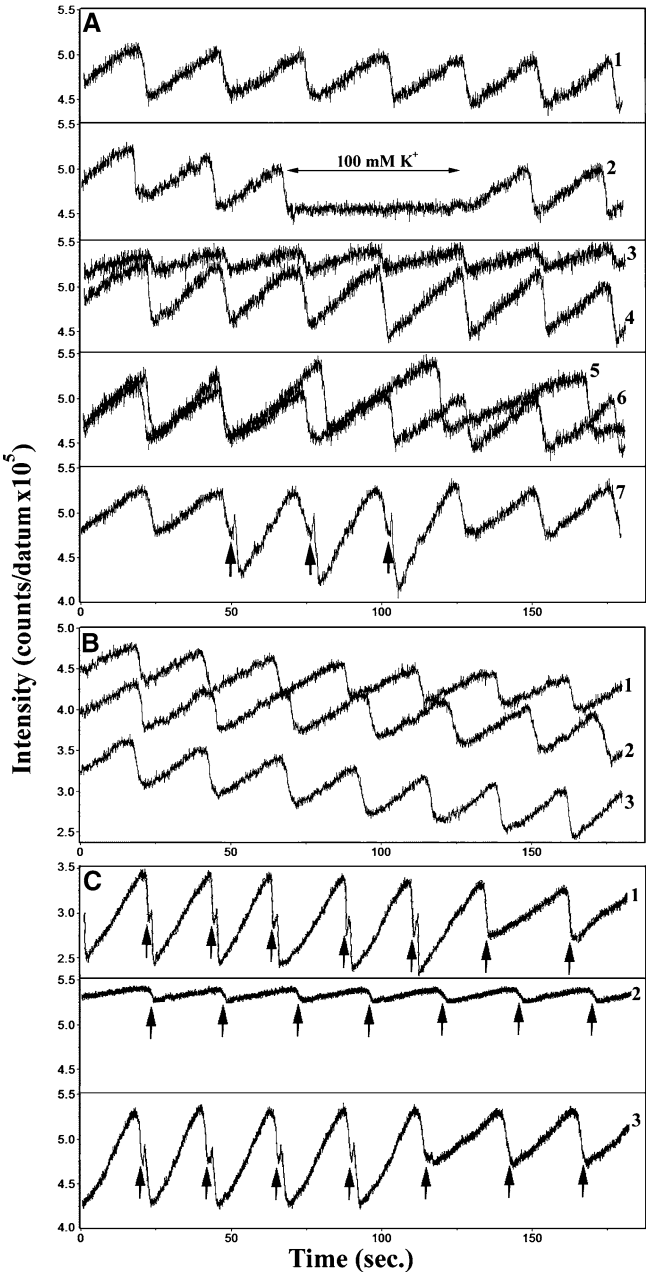

Fig. 7 Analyses of the optical transmembrane potential (OTP) of polarized neutrophils. The OTP of neutrophils was assessed using the fast membrane potential sensitive dye di-8-ANEPPS. The fluorescence emission intensity of di-8-ANEPPS in counts is plotted at the ordinate whereas time (s) is given at the abscissa with a temporal resolution of 20 data points/s. Although intensity changes are proportional to membrane potential changes, some cell-to-cell variability in intensity may be due to differences in loading. **a** Physical properties of the OTP. *Trace 1* shows a representative kinetic evaluation of the OTP, which takes the form of a sawtooth wave with a period of about 20 s Using a flow-through chamber, rapid exchange of the buffer with 100 mM high potassium buffer abolishes the OTP oscillations (*trace 2*). However, the effect is reversible as replacing the medium with a high sodium buffer rapidly restores the properties of the OTP. To better understand the biochemical contributors to the dynamic properties of the OTP, cells were treated with various factors. Ouabain (50 μM) was found to reduce the slope of the sawtooth wave (*trace 3*) vs. control (*trace 4*). In contrast, thapsigargin (0.4 μM) was found to increase the period of the oscillations (*trace 5*) vs. control (*trace 6*). When an electric field was applied during the brief fall in di-8-ANEPPS intensity (depolarization), the depolarization was further enhanced (trace 7). **b** Time-dependent effects of verapamil on di-8-ANEPPS emission intensity. Verapamil at 80 μM was added to cells followed by measurements of the di-8-ANEPPS intensity. To illustrate the time-dependent reduction in di-8-ANEPPS intensity, three measurements of the same cell at different times are overlaid in this panel (*traces 1–3*). *Traces 1*, *2*, and *3* were begun after 10, 15, and 30 min of exposure to verapamil, respectively. The reduction in intensity indicates that the membrane potential is falling during incubation with verapamil. **c** Effects of channel blockers on the OTP response to electric fields. Brief DC pulses were applied as indicated (*arrows*). In *trace 1* the OTP was quantitated after treatment with 80 μM verapamil. Initially, cell responded to electric field application. After >30 min of incubation with verapamil, as ability of the cells to respond to the field disappeared, as indicated at the right hand side of *trace 1*. OTP oscillations were dramatically inhibited by 20 μM mibefradil (*trace 2*). Although 4 μM SKF96365 had no effect on the regular depolarizations of polarized neutrophils, it did block the enhancement of depolarization seen during application of an exogenous electric field. *Trace 3* shows a kinetic study performed immediately after addition of 4 μM SKF96365 to cells. Within 3 min, the cells lost their ability to respond to an electric field

effect of the addition of 50 μM ouabain, a suboptimal dose, on the OTP of polarized neutrophils. It is clear that ouabain reduces the slope associated with the increase in fluorescence intensity (or repolarization). Thus, the amplitude of the OTP changes is regulated by the Na^+/K^+-ATPase. The period of the OTP oscillations appears to be related to the intracellular Ca^{2+} signaling apparatus. Thapsigargin, an inhibitor of the Ca^{2+}–ATPase found in the endoplasmic reticulum, has previously been shown to alter the period of Ca^{2+} oscillations of cells (Visegrady et al. 2001). When a suboptimal dose of 40 nM thapsigargin is added to polarized neutrophils, the oscillation period gradually increases (Fig. 7a, trace 5 vs. the control of trace 6). The OTP of neutrophils oscillates in time with the repolarization of the membrane dependent upon the Na^+/K^+-ATPase and the period phenomenologically associated with the rate of Ca^{2+} entry into the endoplasmic reticulum.

Having confirmed the nature of the OTP oscillations, we next tested the effect of phase-matched electric field exposure and verapamil on OTPs. Although application of an electric field (0.2 V/m) did not have a significant effect on the peak fluorescence intensity of the OTP oscillations (or magnitude of the transmembrane potential), it dramatically enhanced the oscillatory depolarization of the membrane (Fig. 7a, trace 7). One potential explanation is that the electric field is augmenting the entry of charged ions, including Ca^{2+} ions entering via Ca^{2+} channels. Importantly, the timing of the exogenous electric field application (arrowheads in Fig. 7a) coincided with the brief period of membrane depolarization (shown here as a rapid reduction in di-8-ANEPPS fluorescence). The periodic neutrophil membrane depolarization may explain why application of the exogenous electric field must be carefully timed with respect to intracellular oscillators, although this is presently only a correlation.

Using this experimental system, we next tested the hypothesis that verapamil affects the membrane potential of neutrophils. Immediately upon addition to cells, 40 μg/ml verapamil had no effect on the OTP during exposure to electric fields. We found that 40 μg/ml verapamil required approximately 18 min to block the enhanced depolarization mediated by electric fields (data not shown). The effect was dependent upon concentration since 50 μg/ml verapamil required only 15 min and 25 μg/ml verapamil required 35 min (data not shown). Thus, verapamil requires a substantial amount of time to block metabolic resonance. As Kv1.3 is a primary contributor to the K^+ leak current in leukocytes and thereby sets the membrane potential (Leonard et al. 1992; Koo et al. 1997), we checked the time-dependent influence of verapamil on the OTP of cells. Figure 7b, traces 1–3 illustrates the effect of the addition of 40 μg/ml verapamil on the OTP of polarized neutrophils. As this figure shows, the OTP of neutrophils steadily drops over time. However, it is possible that photobleaching might contribute to this reduction in fluorescence intensity. To control for this possibility, di-8-ANEPPS-labeled neutrophils were observed under identical experimental conditions except that verapamil was omitted. Under these conditions, no significant change in fluorescence intensity was observed (data not shown). Thus, the ability of verapamil to block metabolic resonance may be due to its effect on membrane potential. This finding is consistent with the potential role of T-type Ca^{2+} channels as they are functional in a narrow range of membrane potentials.

As the data of Fig. 5 indicate that mibefradil and SKF96365 alter metabolic oscillations in the presence of a phase-matched electric field, we checked the influence of these inhibitors on the OTP of neutrophils. As expected, the addition of 40 μg/ml verapamil had no effect on the electric field-induced enhancement of membrane depolarization (Fig. 7c, trace 1). At 20 μM mibefradil, with or without exposure to electric fields, reduced greatly the amplitude of the OTP oscillations (Fig. 7c, trace 2) within 3 min This suggests that T-type Ca^{2+} channel blockage is not specific for electric field effects and that Ca^{2+} entry plays an important role in mediating the oscillatory depolarization of the membrane. Although addition of 4 μM SKF96365 had no effect on the OTP oscillations, the application of an electric field did not enhance the depolarization of the cell. Furthermore, if 4 μM SKF96365 is added to cells during the application of phase-matched electric fields, within 3 min the cells stop responding to the exogenous field (Fig. 7c, trace 3). Not only does this suggest that a low-dose SKF96365-sensitive channel participates in field sensitivity, but that the response exhibits an all-or-none type of behavior.

Extracellular Ca^{2+}

The inhibitor studies described above indicate that metabolic resonance in an external electric field requires membrane channels and that some of these membrane channels are permeable to Ca^{2+}. This finding suggests that Ca^{2+} entry is important in this process. To test this idea, neutrophils were examined in a flow-through microscope chamber, as described (Albrecht and Petty 1998). When studied in a Ca^{2+}-containing buffer, metabolic resonance was induced in the cells using an appropriately timed electric field (Fig. 8). However, if the Ca^{2+}-containing buffer is washed out by replacing it with an iso-osmotic Ca^{2+}-free buffer, metabolic resonance disappears (Fig. 8). Since the same cell is observed in the presence and absence of an applied electric field and in the presence and absence of a Ca^{2+}-containing buffer, this experiment has internal control experiments. External Ca^{2+} appears to be an important contributor to metabolic resonance in an applied electric field.

Temporal Aspects of Ca^{2+} Signaling and Pharmacological Inhibition

Inasmuch as the several lines of experiments described above implicate the Ca^{2+} signaling apparatus in cellular responses to electric fields, we have directly assessed intracellular Ca^{2+} signals during exposure to electric fields. Repetitive Ca^{2+} spikes have been observed during many neutrophil functions such as migration and phagocytosis (Marks and Maxfield 1990; Maxfield and Kruskal 1987). As these investigators have previously reported, we have observed Ca^{2+} spikes in polarized neutrophils using quantitative microfluorometry. Figure 9a illustrates these Ca^{2+} spikes for an indo-1 labeled neutrophil using a PMT for fluorometric recording. This

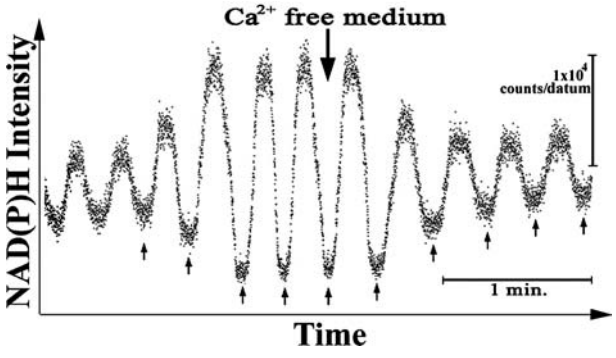

Fig. 8 Metabolic oscillations during application of a phase-matched electric field in the presence and absence of extracellular Ca^{2+}. NAD(P)H autofluorescence intensity in counts (ordinate) is plotted vs. time (abscissa) at a resolution of 20 data points/s. Experiments were performed as described in Fig. 4. A brief DC electric field (0.4 V/m, 200 ms) was applied at the *arrows* shown. NAD(P)H oscillations of the same cell is shown with and without external Ca^{2+} and with and without electric field exposure, thereby forming internal control experiments. Metabolic resonance is observed in the presence of external Ca^{2+}. However, when this medium was replaced with a buffer prepared under Ca^{2+}-free conditions (100 mM NaCl, 20 mM KCl, 5 mM $MgCl_2$, and 4 mM glucose) using a flow-through cell, the high amplitude metabolic oscillations rapidly disappeared despite the presence of an applied electric field. *Bar* = 1 min

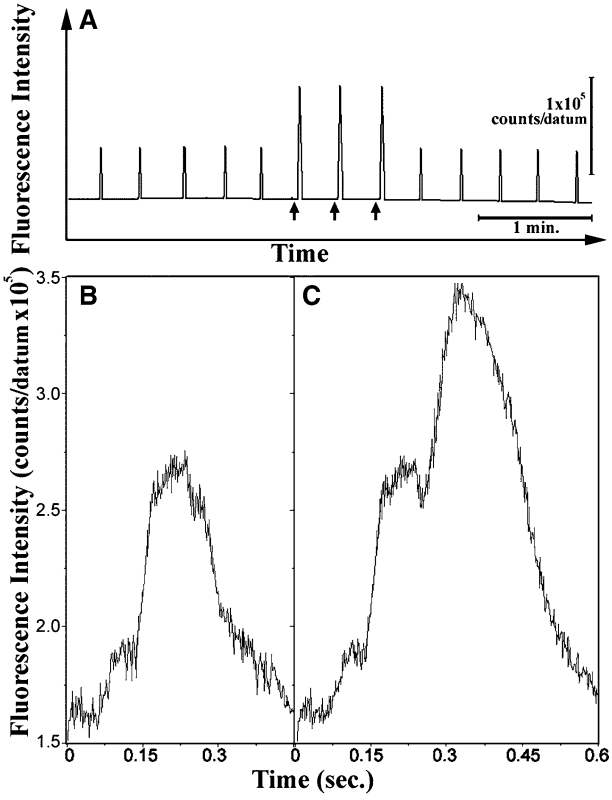

Fig. 9 Ca^{2+} spikes in individual polarized indo-1-labeled neutrophils measured by microfluorometry. In panel A cells were exposed to phase-matched DC electric fields, which were applied at the time points indicated by the arrows. The Ca^{2+} spikes occur at a regular interval of 20 s, as illustrated using a long time-base (10 data points/s) for detection. Importantly, the amplitude of the Ca^{2+} spike dramatically increases during application of a phase-matched electric field. *Bar* = 10^5 counts. To observe the fine structure of these Ca^{2+} spikes, data were also collected using a short time-base (500 data points/s). **b**, **c** Ca^{2+} spikes of cells in the absence and presence, respectively, of a phase-matched electric field. The Ca^{2+} spikes are not symmetrical, but rather have a small shoulder during initiation, a peak, then a decay. During application of an electric field (0.4 V/m, 200 ms), the earlier events resemble those in the absence of an electric field, but the peak intensity is approximately doubled and the total time period covered by the Ca^{2+} spike is greater

shows a series of spikes with an interval of approximately 20 s and a duration of 210 ms We next studied the effects of phase-matched pulsed electric fields on Ca^{2+} signaling. Figure 9a shows an example of Ca^{2+} spikes in untreated polarized neutrophils during application of a phase-matched electric field (arrows). As Ca^{2+} spikes and NAD(P)H oscillations are not temporally aligned, this accounts for field application just prior to the spike (Petty 2000). As these data show, the Ca^{2+} spike becomes significantly more intense and of a somewhat longer duration. As noted for the OTP studies, the Ca^{2+} spike intensity takes on just one value in the presence of a phase-matched electric field, i.e., there are no intermediate values found during electric field treatment. In addition, the Ca^{2+} spikes appeared to develop further structural features during the longer duration. To more clearly identify these changes, experiments were also performed using a shorter time-base. Figure 9b, c shows Ca^{2+} spikes of neutrophils in the absence and presence of an applied electric field, respectively. These experiments illustrate several additional details concerning the Ca^{2+} spike. In the absence of an applied electric field, there is an initial low intensity shoulder followed by an intense peak then a decay in indo-1 intensity. In the presence of a phase-matched electric field, the initial ~200 ms resembles that observed in the absence of a field—a low intensity shoulder followed an intense peak. However, the applied field caused the fluorescence peak to approximately double in intensity during the later stage of the Ca^{2+} spike. Although the Ca^{2+} intensity was altered, there was no change in the Ca^{2+} spike frequency. Therefore, electric field conditions that promote metabolic resonance also promote qualitative changes in the Ca^{2+} spikes of cells. However, the application of an electric field at some other point in time was found to abolish Ca^{2+} spiking behavior (data not shown).

As mibefradil was shown to block metabolic resonance (Figs. 5, 6) at relevant doses, we checked the ability of this drug to influence Ca^{2+} spikes of neutrophils during exposure to phase-matched pulsed electric fields. Cells were studied as described in the previous paragraph except that 1.5 μM mibefradil was added during observations at the point indicated in Fig. 10c. As this figure indicates, within 3 min the Ca^{2+} spikes were reduced to small Ca^{2+} "bumps." Furthermore, after mibefradil treatment, the cells were unable to respond to electric field exposure (Fig. 10d). Thus, this T-type Ca^{2+} channel blocker inhibits Ca^{2+} spikes and Ca^{2+} responses to electric fields.

The ability of SKF96365, an SOC blocker, to influence Ca^{2+} signaling was also tested. However, the dose of SKF96365 that inhibited the normal Ca^{2+} spiking behavior was not the same as the dose that blocked cell sensitivity to electric fields. SKF96365 at 7 μM had no effect on Ca^{2+} spikes (Fig. 10e), but did block cellular detection of electric fields (Fig. 10f). At a slightly higher dose of 10 μM SKF96365, the normal Ca^{2+} spikes (Fig. 10g) as well as Ca^{2+} responses to electric fields were blocked (Fig. 10h). Thus, SKF96365 is acting on at least two sites: at a higher dose Ca^{2+} signals are broadly inhibited whereas at a lower dose cell sensitivity to electric fields is blocked.

Cell polarization

The ability of phase matched electric fields to alter Ca^{2+} spikes (Fig. 10) and waves (see below) suggests that electric fields are affecting cells in a fashion similar to that of receptor ligation. In this and other ways, electric field-treated cells are very much like activated neutrophils. We therefore sought to compare SKF96365-inhibitable behavior of formyl peptide-stimulated cells to that of electric field stimulated cells. We therefore

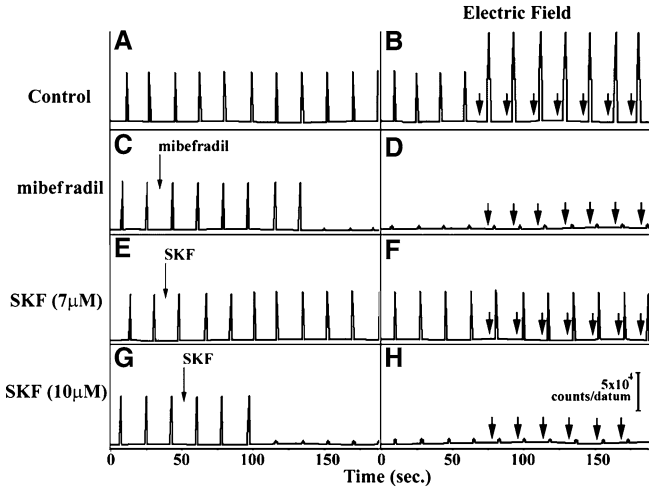

Fig. 10 Effect of mibefradil and SKF96365 on Ca^{2+} spikes of neutrophils in the absence (*column 1*) and presence (*column 2*) of an applied electric field. Indo-1-labeled neutrophils were allowed to polarize on coverslips. Ca^{2+} spikes were followed over time using a microfluorometry apparatus. Data points were collected at 10 s^{-1} Experiments were performed using long time-base to reveal changes in Ca^{2+} spikes over a period of min after addition of reagents (see *arrows*). In the absence of drug addition, Ca^{2+} spikes are observed in neutrophils (**a**), which are enhanced in intensity during application of a phase-matched electric field (0.4 V/m, 200 ms) (**b**). Within 3 min of the addition of 20 μM mibefradil, the Ca^{2+} spikes disappear (**c**) and are replaced by very low intensity "bumps" (**d**). Addition of SKF96365 at 7 μM had no effect on the expected Ca^{2+} spikes (**e**), but blocked the ability of Ca^{2+} spikes to respond to electric fields (**f**). In contrast, a higher dose of SKF96365 (10 μM) rapidly blocked Ca^{2+} spikes (**g**) and electric field sensitivity

measured the percentage of morphologically polarized neutrophils as a function of SKF96365 concentration. In the absence of exogenous stimulants, SKF96365 has no effect upon neutrophil polarization until a dose of about 9 μM is reached. At this dose the cells lose their spontaneous morphological polarization and become spherical in shape. The formyl peptide FMLP binds to the formyl peptide receptor of neutrophils thereby activating cells. When cells were stimulated with 0.5 μM FMLP, a greater percentage of cells became polarized (approximately 70%; Fig. 11) in comparison to unstimulated cells. At about 4 μM SKF96365, the number of polarized cells rapidly fell to the level found for spontaneously polarized cells, i.e., receptor-independent levels. As the dose of SKF96365 is further increased, cell polarization disappears at 9 μM SKF96365, as described above for unstimulated cells. Thus, cell polarization during FMLP stimulation is a multi-tiered response, as is Ca^{2+} signaling. Furthermore, when the percentage of untreated or FMLP-treated cells responding to electric fields is plotted on the same graph (Fig. 11), inhibition of cell responses to electric fields and FMLP both occur at roughly 4 μM SKF96365. Therefore, the SKF96365-sensitive component (such as a TRP(s)) mediating cell sensitivity to applied electric fields resembles that associated with FMLP-mediated stimulation of cell polarization.

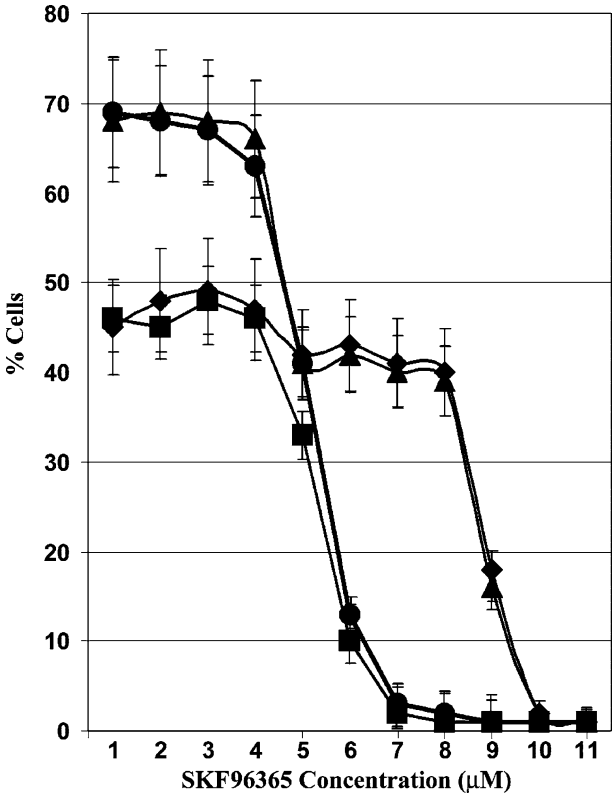

Fig. 11 Effect of SKF96365 on cell polarization and electric field sensitivity. The percent of cells is given on the ordinate and the concentration of SFK96365 is listed on the abscissa. Experiments were performed on spontaneously polarized neutrophils (*filled triangle*, *filled square*) and FMLP-stimulated neutrophils (*filled diamond*, *filled circle*). The percentage of cells demonstrating spontaneous polarization at various SKF96365 concentrations is shown (*filled triangle*); it is inhibited at about 8 μM. In the presence of FMLP more cells become polarized (*filled diamond*). However, the FMLP-induced increase in cell polarization is abolished by 4 μM SKF96365 (*filled diamond*); cell polarization is completely inhibited at 8 μM SKF96365. This dose of SKF96365 also corresponds to the region of inhibition of electric field sensitivity of spontaneously polarized (*filled square*) and FMLP-stimulated cell polarization (*filled circle*)

Spatiotemporal analysis of Ca^{2+} waves

Although quantitative microfluorometry provides detailed temporal information regarding the Ca^{2+} signaling apparatus, it does not provide spatial information. We therefore analyzed the Ca^{2+} spike using high-speed microscopy as previously described (Kindzelskii and Petty 2003; Worth et al. 2003). Extensive control studies have been previously published (Kindzelskii and Petty 2003; Worth et al. 2003). During a Ca^{2+} spike, unstimulated polarized neutrophils display a single Ca^{2+} wave traveling in a counter-clockwise direction (in the laboratory frame of reference as viewed from the basal to apical surfaces) about the perimeter of the cell (Fig. 12a). A previous study has described this Ca^{2+} wave of indo-1-labeled neutrophils in some detail (Kindzelskii and Petty 2003). Using this approach, we divided the Ca^{2+} spikes observed during electric field

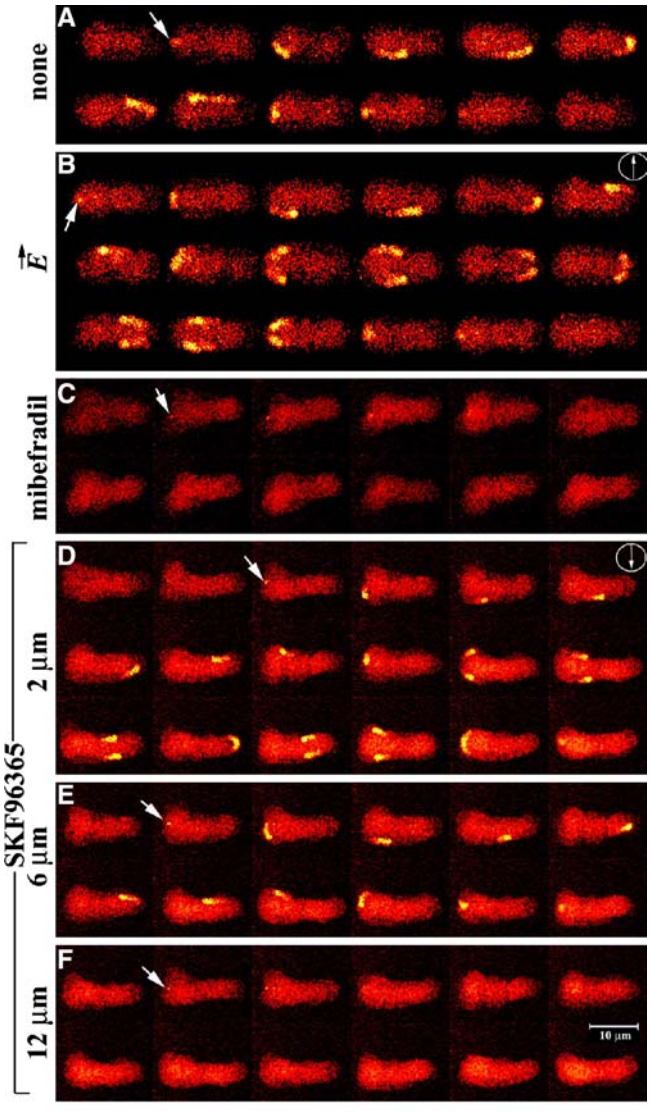

Fig. 12 Spatiotemporal analysis of Ca^{2+} signaling routes using high speed microscopy. Cells were labeled with indo-1 as described above. **a**–**f** Studies of Ca^{2+} wave propagation. Sequential frames are shown from the left to right sides, as a page is read (shutter speed = 250 ns with 20 ms between frames). **a** A Ca^{2+} wave begins at lamellipodium (*arrow*) then rotates about cell periphery. **b** When a phase matched electric field (0.4 V/m, 200 ms) is applied to the same cell as in **a**, a new Ca^{2+} wave is observed. The Ca^{2+} wave begins at the lamellipodium, but when it returns to the lamellipodium, both counterclockwise and clockwise Ca^{2+} waves are seen, which then propagate about the periphery of the cell. As illustrated in **c**, 15 μM mibefradil blocks Ca^{2+} waves, although a brief Ca^{2+} spark can be observed (*arrow*). In view of our findings with SKF96365, we performed high speed imaging experiments at several concentrations of this reagent. At 2 μM SKF96365, no changes in Ca^{2+} waves were detected (**d**). At 6 μM SKF96365 one Ca^{2+} wave was observed in the absence (data not shown) and in the presence of an electric field (**e**). At a higher dose of 12 μM SKF96365, no Ca^{2+} waves could be observed (**f**). Images were collected for 150 ns each. The orientation of the electric field is noted by the *circled arrow* in (**b**) and (**d**). Electric fields were also applied to cells in **e** and **f**, but the cell and the field orientation are identical to those of (**d**). (×760) (*bar* = 10 μm)

exposure into a sequence of 18 spatiotemporal images. In each spike the Ca^{2+} signal begins at the lamellipodium then travels in a counterclockwise direction until it returns to the lamellipodium. At this point in time, the counterclockwise-rotating wave is joined by a clockwise-rotating wave. The Ca^{2+} waves travel in opposite directions about the cell's perimeter then end at the lamellipodium. The formation of this second Ca^{2+} wave is consistent with the all-or-none behavior noted above for the OTP and Ca^{2+} spikes, as well as other observables reported in prior studies (Kindzelskii and Petty 2000; Rosenspire et al. 2000, 2001): either there is sufficient signal to ignite a new Ca^{2+} wave or there is not. The cells in Fig. 12b are becoming elongated due to the accompanying exaggerated cytoskeletal assembly, which we have previously reported during phase-matched field exposure (Petty 2000; Kindzelskii and Petty 2000). Figure 12b also shows that these Ca^{2+} signals are similar of those found for neutrophils immediately after receptor stimulation (Kindzelskii and Petty 2003). During receptor ligation events two waves are observed immediately after ligand binding, which then reverts to a single wave. The phase-matched electric fields of Fig. 12b show two Ca^{2+} waves for each DC field application, whereas only one set of double Ca^{2+} waves are observed after receptor ligation (Kindzelskii and Petty 2003). The Ca^{2+} signaling apparatus is behaving as though it has been independently ligated anew with each field pulse. Another distinction between the effects of DC electric fields and receptor ligation is that the electric field-induced clockwise wave in Fig. 12 always begins at the lamellipodium whereas it begins at the point of receptor ligation in our previous study. This is presumably due to the fact that most of the $K_v1.3$ and some Ca^{2+} channels are clustered at the lamellipodium (Fig. 1) and therefore it is most sensitive to electric fields at this point.

High speed microscopy studies were also performed to better understand the inhibitory mechanisms of mibefradil and SKF96365. When indo-1-labeled neutrophils were studied in the presence of 15 μM mibefradil, no Ca^{2+} wave propagation could be observed (Fig. 12c). Hence, mibefradil inhibits Ca^{2+} signaling before electric field-specific changes in signaling are observed. Therefore, mibefradil may not be acting on a protein(s) associated with electric field detection. Figure 12d–f shows three series of high speed imaging experiments of neutrophils treated with increasing doses of SKF96365 (2, 6, and 12 μM) during application of a phase-matched electric field. Experiments at 2 μM SKF96365 (Fig. 12d) are indistinguishable from control experiments (Fig. 12a). At 6 μM SKF96365 (Fig. 12e) the electric field-specific changes in Ca^{2+} wave propagation disappeared, although propagation of the counter-clockwise wave remained intact. This spatiotemporal finding parallels that noted previously for temporal Ca^{2+} spikes (Fig. 10). A dose of 12 μM SKF96365

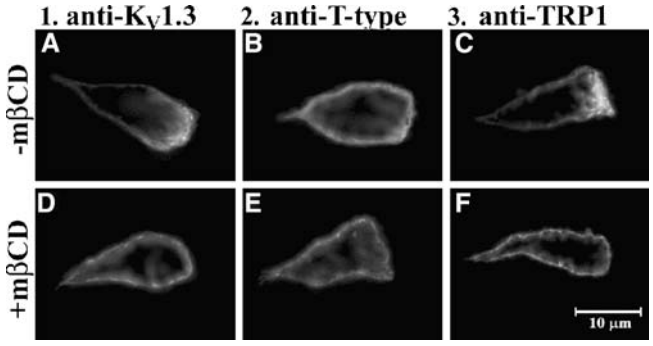

Fig. 13 Effect of mβCD on channel distribution on human neutrophils. Cells were treated with 5 mM mβCD for 15 min at 37°C. Control (**a**–**c**) and mβCD-treated (**d**–**f**) samples were fixed then stained with anti-K_v1.3 (**a**, **d**), anti-T-type channel (**b**, **e**), and anti-TRP1 (**c**, **f**) antibodies as described above. Although mβCD had no effect on the distribution of anti-T-type channel, it caused the redistribution of both K_v1.3 and TRP1 away from the lamellipodium. Each experiment was repeated on at least 8 different days ($n = 8$) with 80 cells scored per for each condition. (×1,020) (*bar* = 10 μm)

blocked both Ca^{2+} waves, suggesting that two different SKF96365-sensitive sites participate in the two Ca^{2+} waves observed.

Effect of mβCD on cellular responses to weak electric fields

The results presented above show clearly that ion channels participate in the detection of weak pulsed electric fields and that ion channels are clustered when cells are responsive. Although morphologically polarized cells cluster K_v1.3 and TRP1 cation channels at the lamellipodium, the relative contributions of morphological polarization and ion channel clustering to electric field sensitivity are unclear. For example, one could argue that morphological polarization is crucial to field detection, not channel clustering. We therefore sought for a means to distinguish the effects of channel clustering from those of morphological changes. Previous studies have shown that lipid rafts play a crucial role in redistributing membrane components during cell polarization and that mβCD inhibits the clustering of many membrane components at the lamellipodium (Manes et al. 1999). Therefore, neutrophils were treated with mβCD under conditions known to disrupt lipid rafts followed by immunofluorescence microscopy. Cells were treated with 5 mM mβCD for 15 min at 37°C. Samples were fixed then stained with anti-K_v1.3, anti-T-type channel, and anti-TRP1 antibodies as described above. Figure 13 shows representative micrographs of neutrophils without and with prior exposure to mβCD. In the absence of mβCD, 92 ± 4% of the cell displayed anti-K_v1.3 clusters at the lamellipodium, 25 ± 6% demonstrated anti-T-type channel clusters, and 88 ± 4% exhibited anti-TRP1 channel clusters. mβCD treatment promotes the redistribution of K_v1.3 and TRP1 away from the lamellipodium (Fig. 12d, f), although the morphological polarization of neutrophils remains intact. Quantitatively, in the presence of mβCD, 4 ± 1.5% of the cells exhibited anti-Kv1.3 clusters, 7 ± 2% expressed anti-T-type clusters, and 11 ± 2% demonstrated anti-TRP1 clusters at the lamellipodium. As expected, mβCD disrupts membrane protein clustering at the lamellipodium.

To evaluate the effects of mβCD at a molecular level, as opposed to the cellular level redistribution noted by microscopic imaging, we next performed emission spectroscopy studies of RET. Figure 14 shows RET spectroscopy on both polarized and spherical neutrophils in the presence and absence of mβCD. As suggested by Fig. 2, RET emission can be detected on both polarized and spherical cells (Fig. 14a, c, respectively). However, treatment with 5 mM mβCD for 15 min at 37°C reduced or eliminated RET on both polarized and spherical cells (Fig. 14b, d). RET could be restored to ≥75% of the mβCD-treated cells by incubation with autologous serum containing 50 mg/ml exogenous cholesterol for 20 min at 37°C (data not shown). Thus, mβCD was very effective at disrupting membrane clusters at both the cellular and supramolecular structural levels. As spherical cells were not sensitive to weak electric fields but were positive for RET, neutrophils apparently require membrane clusters greater than 10 nm in size to detect electric fields.

As K_v1.3 and TRP1 participate in Ca^{2+} signaling, we ascertained the effect of mβCD treatment on Ca^{2+} spikes of morphologically polarized neutrophils. As previously mentioned, polarized neutrophils display Ca^{2+} spikes at approximately 20 s intervals (Fig. 15a),

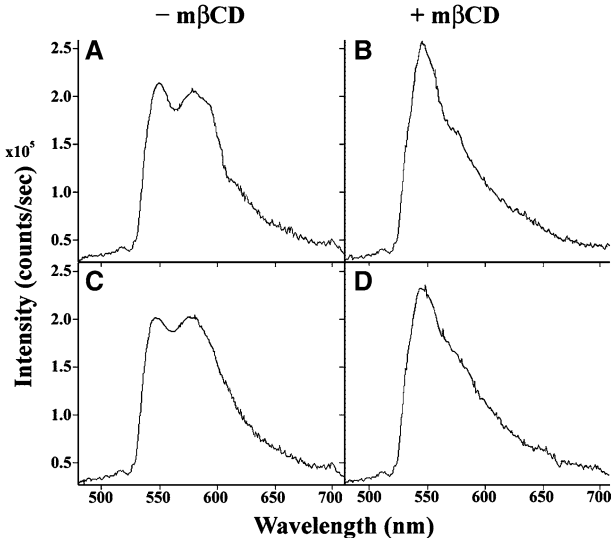

Fig. 14 mβCD reduces RET between TRITC-anti-K_v1.3 and FITC-anti-TRP1. Experiments were performed as described in Fig. 3. The wavelength (nm) is shown at the abscissa whereas the emission intensity (counts/s) is given at the ordinate. Both polarized (**a**, **b**) and spherical (**c**, **d**). Untreated (**a**, **c**) and mβCD-treated (**b**, **d**) cells are shown. RET is dramatically reduced by mβCD

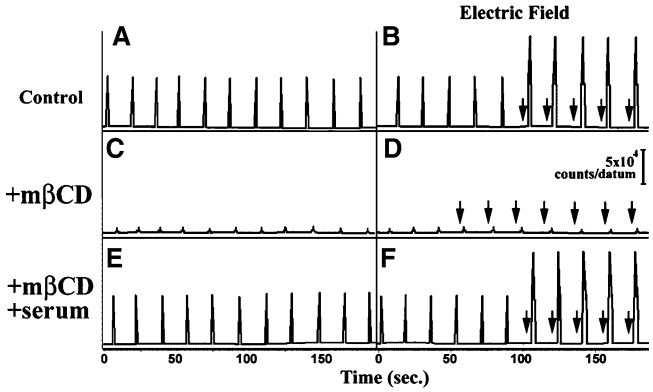

Fig. 15 Effect of mβCD on Ca^{2+} spikes in the presence and absence of electric fields. The Ca^{2+} intensity (ordinate) is plotted vs. time (abscissa) at 10 data points/s Cells unexposed to an electric field are shown at the *left hand side* (**a**, **c**, **e**). A DC electric field (0.4 V/m, 200 ms) was applied to cell at the arrows (*right hand side*; **b**, **d**, **f**). Control cells show enhanced Ca^{2+} spikes (**d**). Cells treated with mβCD displayed low-intensity Ca^{2+} "bumps" (**c**) and did not demonstrate heightened amplitudes in the presence of a phase-matched electric field (**e**). However, normal Ca^{2+} signals could be restored after mβCD-treated cells were incubated with serum and cholesterol (**f**)

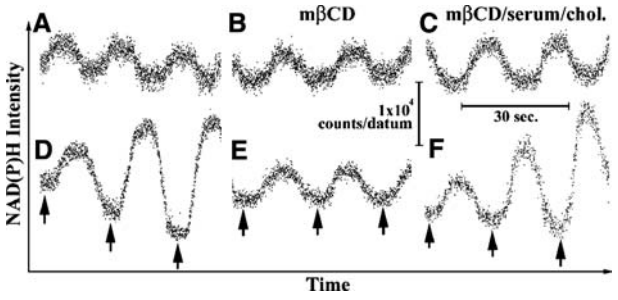

Fig. 16 Effect of mβCD on metabolic oscillations in the presence and absence of electric fields. The NAD(P)H autofluorescence intensity (ordinate) is plotted vs. time (abscissa) at 20 data points/s Cells unexposed to an electric field are shown in the top row (*traces a–c*). A DC electric field (0.4 V/m, 200 ms), was applied to cell at the *arrows* (*bottom row*; *traces d–f*)). Control cells show metabolic resonance (*trace d*). Cells treated with mβCD continued to display NAD(P)H oscillations (*trace b*), but did not demonstrate heightened oscillatory amplitudes in the presence of a phase-matched electric field (*trace e*). However, metabolic resonance could be restored after mβCD-treated cells were incubated with serum and cholesterol (*trace f*)

which are substantially increased in amplitude in the presence of a phase-matched electric field (Fig. 15b). However, treatment with mβCD dramatically reduces the intensity of Ca^{2+} spikes to Ca^{2+} "bumps" in both the absence and presence of an applied phase-matched electric field (Fig. 15c, d). Thus, mβCD exposure leads to the redistribution of plasma membrane's Ca^{2+} signaling apparatus and, concomitantly, disrupts the Ca^{2+} signals previously associated with cell polarization and electric field exposure. Furthermore, the effects of mβCD were reversible, as incubation of mβCD-treated cells with autologous serum containing 50 mg/ml cholesterol for 20 min at 37°C restored normal Ca^{2+} signals (Fig. 15e,f).

We next evaluated the effect of mβCD exposure on metabolic oscillations. As previously described (Kindzelskii and Petty 2000), electric fields appropriately timed to coincide with certain intracellular chemical oscillations enhance the amplitude of NAD(P)H oscillations in morphologically polarized cells (Fig. 16d). However, this is not observed in mβCD-treated cells (Fig. 16e). The loss of metabolic resonance is not likely explained by cell toxicity. First, cell metabolism and metabolic oscillations remain intact for treated cells (Fig. 16b). Second, no irreversible changes in cell sensitivity were caused by mβCD treatment, as mβCD-treated cells incubated with ~90% autologous serum containing 50 mg/ml exogenous cholesterol for 20 min at 37°C could respond to electric fields (Fig. 16f). Moreover, at least a portion of the Ca^{2+} signaling machinery remained intact in mβCD-treated cells (see below). It would therefore appear that ion channel clustering at a relatively large scale, not cell polarization, is a key factor in neutrophil detection of weak electric fields.

MPO trafficking in metabolic resonance

Although the above studies have outlined the roles of ion channel clustering in cell responses to weak phase-matched electric fields, they do not account for the enhanced oscillatory NAD(P)H amplitudes (metabolic resonance). We therefore sought to tie the oscillatory changes previously described (e.g., Kindzelskii and Petty 2000) and illustrated above (e.g., Fig. 5) with the signal transduction apparatus. As MPO promotes heightened NAD(P)H amplitudes in neutrophils (Olsen et al. 2003), we tested the hypothesis that MPO trafficking participates in electric field-mediated perturbation of cell metabolism. In the first series of experiments, cells were treated with a panel of MPO inhibitors (Davies and Edwards 1989; Jerlich et al. 2000). These inhibitors included SHA, pHBAH, HQ and cyanide. For example, neutrophils were treated with 50 mM SHA for 20 min at 37°C followed by experimentation. Although SHA had no effect on control cells not treated with electric fields, this MPO inhibitor did block the ability of cells to undergo metabolic resonance in the presence of a phase-matched electric field (Fig. 17). This effect, however, was not specific for SHA as a panel of MPO inhibitors including pHBAH, HQ, and cyanide had a similar effect (Fig. 17). This suggests that MPO participates in metabolic resonance.

One factor believed to be important in the formation of high amplitude metabolic oscillations is the delivery of MPO and the NADPH oxidase to the same cellular compartment (Olsen et al. 2003). As the NADPH oxidase can be found at the cell surface and MPO can be delivered to the cell surface in the presence of certain stimuli, we tested the cellular disposition of MPO in the presence and absence of stimulation with an electric field. When the cells were fixed, both untreated and electric field-treated cells displayed staining within the

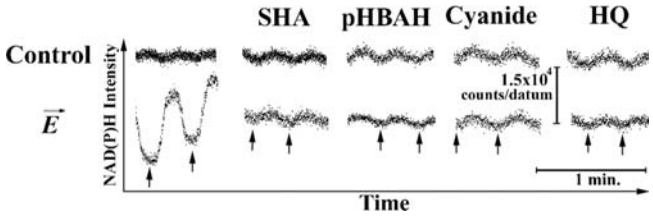

Fig. 17 Effect of myeloperoxidase (MPO) inhibitors on metabolic oscillations in the presence and absence of electric fields. The NAD(P)H autofluorescence intensity (ordinate) is plotted vs. time (abscissa) at 20 data points/s Cells unexposed to an electric field are shown in the top row. A DC electric field (0.4 V/m, 200 ms), was applied to cells shown in the *bottom row*. Cells were treated with no MPO inhibitor (*column 1*), 50 μM salicylhydroxamic acid (SHA) (*column 2*), 50 μM p-hydroxybenzoic acid hydrazide (pHBAH) (*column 3*), 10 mM cyanide (*column 4*) or 1.5 mM hydroxyquinone (HQ) (*column 5*). Although untreated cells show metabolic resonance, cells treated with any of the various MPO inhibitors did not display heightened NAD(P)H oscillations

cytoplasm and in the proximity of the surface as judged by immunofluorescence microscopy (Fig. 18). To evaluate the surface expression of MPO, live cells were observed and stained with the anti-MPO antibody. When examined by fluorescence microscopy, live untreated cells were not stained by anti-MPO (Fig. 18). However, cells exposed to a phase-matched electric field were stained with the anti-MPO reagent, although nearby cells on the microscope slide were unstained. However, cells exposed to phase-matched electric fields could not be stained with antibodies directed against another metabolic enzyme, lactate dehydrogenase (data not shown). MPO possesses a high positive charge and thereby may electrostatically bind to the cell. To test this idea, control cells or cells treated with phase-matched electric fields were washed with a hypertonic (400 mM NaCl) for 40 s while adherent to microscope slides. Following this treatment, MPO could not be detected at the cell surface. To link these findings to our previous finding that the calcium signaling inhibitor SKF96365 blocks metabolic resonance, we tested the ability of cells treated with this reagent, as described above, to block the appearance of MPO at the cell surface during exposure to phase-matched electric fields. As illustrated in Fig. 18, exposure to SKF96365 blocks both cell extension as well as anti-MPO labeling of the cell surface in response to electric fields. Therefore, MPO trafficking to the cell surface appears to contribute to metabolic resonance.

Fig. 18 Anti-MPO labeling of fixed and living human neutrophils. Cells were either not exposed to phase-matched electric fields (*columns 1* and *2*) or exposed to electric fields (*columns 3* and *4*). In *row 1*, cells were fixed with 3.7% paraformaldehyde prior to labeling. In both the presence and absence of electric field treatment, extensive labeling of the cytoplasm of all cells can be noted. Significant labeling of the cell surface with anti-MPO was not observed under any condition for cells not treated with a phase-matched electric field (*columns 1* and *2*). However, live cells exposed to an electric field (0.4 V/m, 200 ms) were stained at the cell surface with anti-MPO, although a neighboring cell not phase-matched with the applied field was not stained. MPO staining disappeared after a high salt washing procedure, which presumably dislodges electrostaically bound MPO from the cell. Furthermore, incubation with SKF96365, which blocks metabolic resonance (Fig. 4), also blocks MPO appearance at the plasma membrane of cells exposed to electric fields. (*bar* = 10 μm)

Based on these findings, we next sought to reconfirm the role of MPO in metabolic resonance using other approaches. In the first experiment, we added purified MPO (10 μg/ml) to untreated neutrophils. As expected, the amplitude of the metabolic oscillations increased dramatically (Fig. 19). Moreover, if MPO is removed from the surface of cells using the salt wash protocol mentioned in the preceding paragraph, the NAD(P)H amplitudes returned to a normal level (Fig. 19). Therefore, several lines of evidence support the idea that MPO trafficking contributes to the calcium signal-mediated initiation of metabolic resonance.

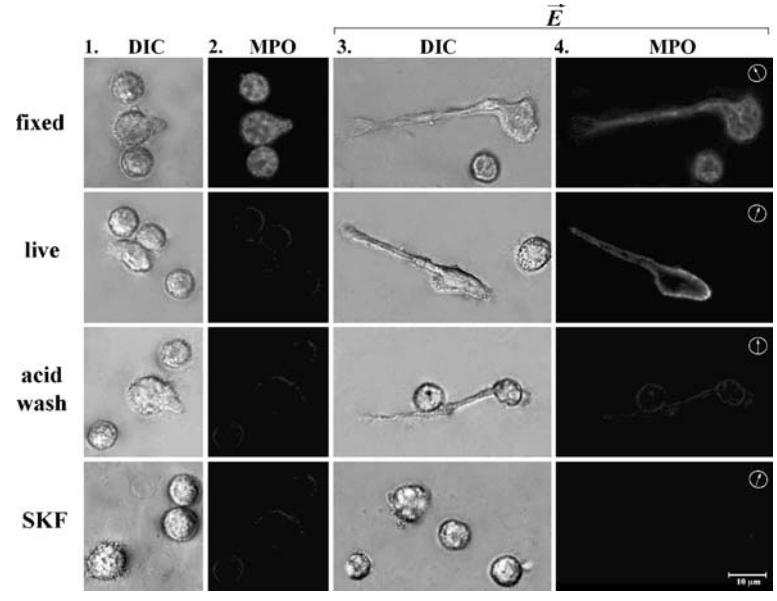

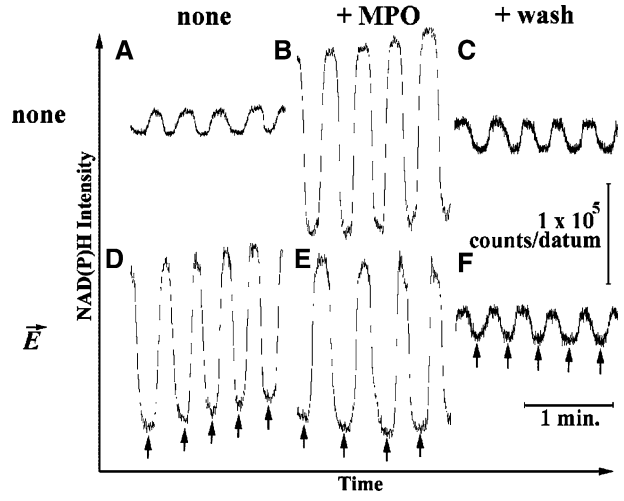

Fig. 19 Effect of surface MPO on metabolic oscillations in the presence and absence of electric fields. The NAD(P)H autofluorescence intensity (ordinate) is plotted vs. time (abscissa) at 10 data points/s. Cells unexposed to an electric field are shown in the *top row* (*traces a–c*). A DC electric field (0.4 V/m, 200 ms), was applied to cells (*bottom row*; *traces d–f*)). The metabolic amplitude of cells not exposed to electric fields, but incubated with MPO was increased. On the other hand, the metabolic oscillation intensity could not be further increased in electric field treated cells when incubated with MPO. High salt washes had no effect on untreated cells whereas they reduced the amplitudes of cells exposed to electric fields

Discussion

In the present study we have shown that ion channel clusters participate in the detection of weak electric fields by polarized human neutrophils. Although the functional abilities of both K^+ and Ca^{2+} channels appear to contribute to cell sensitivity to electric fields, the role of the K^+ channels appears to be secondary to their ability to influence the transmembrane potential of neutrophils. Low voltage T-type Ca^{2+} channels participate in an early step in Ca^{2+} signaling. However, as revealed by the spatiotemporal imaging of Ca^{2+} waves, mibefradil blocked Ca^{2+} signaling before electric field-mediated changes in Ca^{2+} amplitude and wave propagation patterns. Consequently, T-type channels may constitute a requisite step in electric-field induced Ca^{2+} signaling, but may not play a direct role in field detection. However, SKF96365 dose–response studies of neutrophil behavior in the presence of weak electric fields indicated that 6 μM SFK96365 blocked electric field-mediated changes in cell signaling without blocking metabolic oscillations or other Ca^{2+} signals normally present in human neutrophils. Therefore, multiple membrane channels participate at multiple levels in the detection of weak electric fields. Furthermore, the channels are only capable of detecting electric fields when found in a cluster at the lamellopodium of cells. One consequence of SKF96365-sensitive Ca^{2+} signaling is the translocation of MPO from intracellular stores to the plasma membrane, where MPO promotes enhanced metabolic amplitudes (Olsen et al. 2003).

Ion channel clustering and the Galvanovskis and Sandblom prediction

A central element of the theoretical analysis of Galvanovskis and Sandblom (1997) is that cells exhibiting clusters of ion channels are far more sensitive to electric fields than cells with uniformly distributed channels. The ability of ion channels to exhibit clustering is well known in biological systems. Previous studies have demonstrated channel clusters on other polarized cells including arterial endothelium, photoreceptor synapse, olfactory neurons, muscle cells, cochlear outer hair cells and protoplasts (Shaw and Quatrano 1990; Goligorsky et al. 1995; Nachman-Clewner et al. 1999; Schild et al. 1995; Oshima et al. 1996; Vallee et al. 1997). The present study has demonstrated that polarized neutrophils, which are sensitive to weak electric fields, demonstrate clusters of $K_v1.3$ channels and TRP1 channels whereas spherical neutrophils are not sensitive to electric fields and do not exhibit large channel clusters. This comparison is particularly strong because it is the same cell type in the presence and absence of ion channel clustering; the differences cannot therefore be accounted for by cell-to-cell variations. However, both morphological polarization and ion channel clustering accompany cell sensitivity to weak electric fields. To test the relative roles of morphological polarization and ion channel clustering, ion channel clusters were disrupted using mβCD (see below), which also blocked field detection without altering cell viability. Thus, several lines of evidence presented above are consistent with the prediction of Galvanovskis and Sandblom (1997) concerning the role of ion channel clustering and electric field sensitivity. Furthermore, we have provided a rational mechanism of channel clustering, identified the role(s) of several participating channel types, identified the oscillations in membrane potential as a key factor in determining the timing of electric field application, and suggested further theoretical avenues for exploration.

Biochemical mechanism of channel clustering

Our work has shown that $K_v1.3$ and TRP1 are clustered at the lamellipodium of morphologically polarized neutrophils. The redistribution of these membrane proteins to the leading edge of the cell was dramatic. However, several other molecules have been shown to undergo dramatic re-organizations during neutrophil polarization, including the urokinase-type plasminogen activator receptor and complement receptor type 4 (Kindzelskii et al. 1997). Therefore, it is not surprising that some membrane proteins may accumulate at the lamellipodium. Recent studies have shown that $K_v1.5$, TRP1, K_{vCa}, and Na channels are associated with lipid rafts

(Martens et al. 2001; Brazer et al. 2003; Lockwich et al. 2000; Bravo-Zehnder et al. 2000; Hill et al. 2002). Furthermore, recent studies have shown that lipid rafts accumulate at the lamellipodium of morphologically polarized cells (Manes et al. 1999). Therefore, one might anticipate that certain membrane channels would form clusters on leukocyte membranes. Indeed, we have found this to be the case with $K_v1.3$ and TRP1 accumulating at the lamellipodia of neutrophils. The formation of these channel clusters has been postulated to be due to the formation of cholesterol-rich lateral phase separations in cell membranes (Pike 2003; Silvius 2003). Lipid rafts have been proposed as signal transduction platforms to mediate a variety of biological signaling events, especially in immune cells (Dykstra et al. 2003); thus, both the ion channels and the cellular signaling apparatus, including its intracellular elements, are strategically clustered at the lamellipodium. Using mβCD, which has been reported to disrupt lipid rafts, we could randomize membrane channels about the periphery of the cell and, in parallel, block the effects of phase matched electric fields on cells including Ca^{2+} signaling and metabolic resonance. Moreover, the effects were reversible by delivery of cholesterol to cells, which presumably reconstitutes lipid rafts. Furthermore, TRP channels, due to their oligomerization, ankyrin-like repeats, and calmodulin binding sites, also serve as key signaling platforms in cells. Thus, the lamellipodium is a key site for signaling in polarized neutrophils. Not only do these findings provide the biological basis for channel clustering, but they may also account for why electric fields induce Ca^{2+} waves at the lamellipodium, but not at any other location on the plasma membrane (e.g., Fig. 12b).

Nature of the membrane channels involved in field detection

Over the past decade there has been much interest in identifying the ''primary field detector'' responsible for the effects of weak electric fields on cells. Our works suggests that weak electric field sensitivity is not the province of any one channel or type of channel, but rather a collective property of many channels. Field detection is an emergent property that involves millions of channels within a cluster interacting with the applied field, their surroundings and one another, as well as their coupling with intracellular oscillators.

Ca^{2+} signaling has been previously suggested to participate in the detection of weak electric fields (Walleczek and Liburdy 1990; Uckum et al. 1995; Yost and Liburdy 1992; Lindstrom et al. 1995; Lyle et al. 1988, 1991), although some controversy has surrounded these claims. One of the reasons for the controversy has been the lack of a robust experimental observable. As we have previously pointed out (Kindzelskii and Petty 2000), by applying the electric field at specific intervals corresponding to certain intracellular oscillations within a specific time frame (see below), robust biological effects were found. We therefore could test the effects of various channel blockers on the cellular responses to electric fields. The well-known phenylalkylamine verapamil was found to block metabolic resonance. Verapamil is best known for its ability to bind to L-type Ca^{2+} channels. However, the L-type channel blocker nifedipine did not affect cells at relevant doses. Furthermore, the dose of verapamil required to block metabolic resonance was found to be substantially higher than that required to block L-type channels. However, this dose was consistent with that required to block K^+ channels (Robe and Grissmer 2000; Rauer and Grissmer 1999). Verapamil has been found to block several neutrophil functions (e.g., Haga et al. 1996; Irita et al. 1986; Simchowitz and Spilberg 1979). When the well-known K^+ channel inhibitors TEA and 4-AP were evaluated, they were found to block metabolic resonance at pharmacologically-relevant doses, clearly implicating K^+ channels in weak electric field detection. Although more specific and powerful K^+ channel inhibitors have been discovered, the sale of certain of these reagents in the U.S.A. has been restricted due to their potential use as bioterrorism agents due to their potent toxicity. However, kinetic studies revealed that approximately 20–30 min was required for verapamil to block metabolic resonance. Although K^+ channels were clearly involved at some level, they did not seem to block early events in field detection. As K^+ leakage sets the membrane potential (Leonard et al. 1992; Koo et al. 1997), prolonged incubation with K^+ channel blockers would be expected to reduce the membrane potential, which in turn could affect transmembrane signaling events such as Ca^{2+} entry. We discovered that this was the case. Measurements of the OTP of neutrophils incubated with verapamil decreased over time. This decrease could not be accounted for by photobleaching the probe employed in these experiments. Therefore, K^+ channels appear to influence the detection of weak electric fields only after they have substantially reduced the transmembrane potential of leukocytes. As multiple types of K^+ channels collect at lipid rafts ($K_v1.5$, $K_v1.3$, K_{vCa}, and likely others), we have not yet established which channel is responsible for the reduction of the membrane potential and metabolic resonance.

As the transmembrane potential is a key contributor to the electrochemical gradient driving Ca^{2+} into cells, we further analyzed the role of membrane Ca^{2+} channels. Although Ca^{2+} channel blockers such as nifedipine inhibited metabolic resonance, the doses required were thousands of times higher than that required to block their Ca^{2+} channel targets (L-type channels), indicating that the inhibition was non-specific. However, mibefradil, a low-voltage activated T-type Ca^{2+} channel blocker, was found to inhibit metabolic resonance at pharmacologically-relevant doses. This indicates that T-type channels participate in transducing electric field stimulation into metabolic changes. Furthermore, since T-type Ca^{2+} channels are only functional within a narrow range of voltages (Perez-Reyes 2003), it seems

reasonable that perturbations of the membrane potential with K^+ blockers would influence T-type channel activity. However, when the effects of mibefradil on Ca^{2+} signaling were more closely evaluated, it was found to inhibit more than the electric field-induced changes in the Ca^{2+} signaling apparatus. In the absence of an electric field, mibefradil reduced the Ca^{2+} spikes to small Ca^{2+} "bumps." Furthermore, when Ca^{2+} signals were evaluated by high-speed microscopy (Kindzelskii and Petty 2003; Worth et al. 2003), the Ca^{2+} wave normally present in morphologically polarized neutrophils was absent; it was replaced by a brief Ca^{2+} spark at the lamellipodium, presumably the physical counterpart of the temporally measured "Ca^{2+} bump." An absence of Ca^{2+} wave propagation in mibefradil-treated neutrophils is consistent with the pericellular location of T-type Ca^{2+} channels. Mibefradil appears to inhibit metabolic resonance at a step prior to electric field signal transduction changes. Thus, T-type channels are a necessary condition, but their direct role in field detection is indeterminate.

SOCs are an important component of the neutrophil transmembrane signaling apparatus for cell activation (Itagakin et al. 2002). As the Ca^{2+} wave triggered by electric field application resembled in speed, direction and intensity the Ca^{2+} wave association with neutrophil activation (Kindzelskii and Petty 2003), we examined the role of SOCs in cellular responses to electric fields. At saturating doses, the SOC channel blocker SKF96365 was found to inhibit the propagation of Ca^{2+} waves, as noted for mibefradil. However, at lower doses of SKF96365 it was possible to inhibit the electric field induced Ca^{2+} wave while maintaining the counter-clockwise traveling Ca^{2+} wave. In parallel, at a concentration of 10 μM, neutrophils were unable to undergo spontaneous morphological polarization and migration. SKF96365 at 5 μM eliminated the FMLP-induced enhancement in cell polarization without affecting spontaneous polarization. Furthermore, the Ca^{2+} spikes and the counter-clockwise propagating Ca^{2+} wave associated with morphological polarization were intact. When neutrophils exposed to 5 μM SKF96365 were treated with electric fields, the cells were unable to respond. Thus, there appears to be at least two SKF96365 binding affinities, likely associated with different SOCs. One of these sites is associated with cell polarization while the second contributes to Ca^{2+} wave propagation in the presence of the first Ca^{2+} wave and an activation signal, such as FMLP or an appropriately timed electric field. It seems likely that SOCs are part of a complex of plasma membrane proteins whose activity can be affected by weak electric fields.

Several SOCs are members of the TRP family of gene products. Several TRPs have been demonstrated at the protein and/or mRNA levels in leukocytes (Gamberucci et al. 2000). TRP1 is one of the best characterized TRP family members (Minke and Cook 2002). We have found that TRP1 is clustered at the lamellipodium of cells. Although TRP1 protein has been detected in leukocytes (Mori et al. 2002; Vazquez et al. 2001), TRP1 message was not observed in neutrophils (Heiner et al. 2003). As there is little genetic activity in neutrophils (the nucleus is condensed, hence the name polymorphonuclear leukocytes) or protein turnover (neutrophils live for only 3 days in the peripheral blood), an absence of message has no bearing on the presence of TRP1. As pointed out above, TRP1 is a lipid raft-associated protein (Lockwich et al. 2000; Trevino et al. 2001) and the lamellipodium is enriched in lipid raft-associated proteins, the clustering of TRP1 at this site is expected. Moreover, since there are ~20 members of the TRP supergene family, it would not be surprising that these multiple TRP proteins explained the two-tiered dose–response properties of SKF96365 on neutrophils. It would appear that two or more TRP proteins participate in neutrophil Ca^{2+} signaling. It seems likely that TRP1 or one of its homologues participates at a very early step in the detection of weak electric fields.

Table 1 summarizes the roles of membrane channels in cell responses to weak electric fields. Briefly, extracellular Ca^{2+} appears to play a role in the cellular detection of weak electric fields because metabolic resonance can be eliminated by washing Ca^{2+} out of the bathing solution. As Ca^{2+} is not required for the morphological polarization of neutrophils (Marks and Maxfield 1990), the effect could not be due to lack of cell polarization. However, verapamil did not inhibit metabolic resonance due to its effect on Ca^{2+} channels, but rather an effect on K^+ channels. K^+ channel inhibitors apparently influenced metabolic resonance via their role in setting the membrane potential, which in turn affects Ca^{2+} entry. T-type Ca^{2+} channels are required for electric field detection, but may play more of a supporting role than actually responding to the field. SOCs are the earliest membrane channels that we have found which participate in field detection. This is consistent with the recent study of Trollinger et al. (2002) showing the Gd^{3+}, which blocks SOCs, inhibits galvanotaxis; this raises the possibility that SOCs are broadly relevant to electric field-cell interactions. Importantly, the K^+ channels and SOCs are strategically clustered at the lamellipodium, as shown by the ability of lipid raft inhibitors to reorganize the distribution of these channels and abolish sensitivity to electric fields.

Chemical oscillators and the timing of field application

Chemical oscillations are a well-known feature of many cell types, including neutrophils (Petty 2001). Membrane potential, metabolism, intracellular Ca^{2+} concentrations, superoxide production, pericellular proteolysis, cell shape, velocity and other properties are known to oscillate in polarized neutrophils. Prior theoretical (Galvanovskis and Sandblom 1997; Eichwald and Kaiser 1993, 1995) and experimental (e.g., Lindstrom et al. 1995; Lyle et al. 1991) studies have suggested that Ca^{2+} signaling participates in cellular detection of weak

Table 1 Contributors to the detection of weak electric fields

Structure	Inhibitor	Proposed role
K_v	Verapamil, TEA, 4-AP	Membrane potential
T-type	Mibefradil	Calcium wave propagation
SOCs	SKF96365 (6 μM)	Ignition of electric field-sensitive calcium wave
	SKF96365 (12 μM)	Propagation of both calcium waves
Extracellular calcium	EDTA	Calcium entry
Lipid rafts	mβCD	Assembly of ion channel clusters

electric fields. However, experimental studies have generally applied electric fields to large populations of cells followed by bulk assays, which necessarily discards all of the oscillatory and phase information associated with both the electric field and the oscillatory chemistry of each individual cell. Our earlier work has stressed the importance of electric field frequency and phase with respect to intracellular chemical oscillators (Kindzelskii and Petty, 2000). Therefore, we have carefully frequency- and phase-matched electric field application with intracellular oscillators and obtained robust findings concerning the roles of ion channels in electric field detection.

Previous publications from this laboratory have shown that when a brief DC electric field is applied during a trough in the NAD(P)H oscillation, the NAD(P)H oscillations, as well as Ca^{2+} oscillations and other parameters, grow in amplitude (Kindzelskii and Petty 2000; Petty 2000). Although cellular responses correlated with the NAD(P)H trough, it does not mean that the applied field was acting by directly affecting cell metabolism. During the course of these studies, we discovered another cellular variable that correlated strongly with timing of electric field sensitivity: the transmembrane potential. Although the applied electric field is likely too weak to register as a change in transmembrane potential, the applied field affects the slope of the periodic membrane depolarization leading to greater depolarization of the membrane (Fig. 7a, trace 7). The enhanced oscillatory depolarization is completely consistent with the enhanced cation entry during exposure to electric fields. In our experiments the phase-matched DC electric field was applied just before the Ca^{2+} peak, which is during the periodic membrane depolarization—but before the depolarization is complete. When the fluorescence reaches its minimum intensity (maximal depolarization), the Ca^{2+} intensity has reached its peak intracellular concentration. If the electric field is applied at some other point in the oscillatory cycle, cells do not respond with enhanced Ca^{2+} entry and metabolic changes. This change in the oscillatory transmembrane potential is, like the change in Ca^{2+} wave patterns, one of the earliest effects specific for applied electric fields. Interestingly, it seems to appear at the time that would have corresponded roughly to the depolarization trough, had the field not been applied. This may correspond to the time when two Ca^{2+} waves appear during exposure to the applied electric field.

Emergent properties of channel clusters

Our findings are consistent with certain features of the Galvanovskis and Sandblom (1997) model of cell interactions with weak electric fields. In this paper they report a signal-to-noise (S/N) ratio of 0.3, which is somewhat low, but an improvement over earlier theoretical treatments. As previously mentioned, channels form small clusters in lipid rafts of spherical cells and large clusters at the lamellipodium of neutrophils. As spherical cells may display RET but not electric field sensitivity, then the effective clusters must be large in size. If a TRP family member is an early component in field detection, then small microscopic clusters (Fig. 2l) may be below the detection threshold. Galvanovskis and Sandblom (1997) anticipated much smaller channel clusters of 10^2–10^3 channels. As the S/N ratio goes as the square root of N and the number of the channels at the lamellipodium is $\sim 10^6$, a polarized cell will have a S/N ratio $\sim$30 (which may be further improved using our smaller signal frequency). Clusters several μm in size containing $\sim 10^6$ channels are associated with weak field detection. The S/N estimate of Galvanovskis and Sandblom (1997) may be low due to the conservative estimate of channel numbers, at least with respect to the neutrophil system.

In addition to channel clustering, other mechanisms of amplification may participate in the detection of weak electric fields. For example, if the clusters have regions of densely packed ion channels, channel-to-channel cooperativity may provide further amplification (Duke and Bray 1999). Neumann (2000) has recently discussed electric field detection in the presence of channel cooperativity. Furthermore, allosteric modulation of ion channels is an emerging theme in biology (Rothberg 2004). One integral requirement for cooperative interactions among proteins is their molecular proximity. Although we have not formally demonstrated cooperativity among ion channels, our RET experiments show that these channels are less than $\sim$7 nm from one another. Since this is the approximate size of a channel, this suggests that ion channels can form nearest neighbor complexes and, therefore, could display functional cooperativity. This would also be consistent we our earlier study showing a threshold effect in electric field sensitivity, as evidenced by a sigmoidal dose–response curve (Kindzelskii and Petty 2000), which is a widely-recognized feature of systems exhibiting cooperativity.

Furthermore, the all-or-none type of behavior exhibited by this system is consistent with reaching a threshold that supports the propagation of a Ca^{2+} wave. Our high speed fluorescence microscopy experiments show that phase-matched electric field application causes Ca^{2+} entry at the lamellipodium (Fig. 12). However, Ca^{2+} entry occurs simultaneously from a large region of the lamellipodium, suggesting that the channels are operating in unison-consistent with a cooperative mechanism. In addition to the idea of channel-channel interactions mediated by a conformational spread, channel-to-channel communication is also provided by Ca^{2+}. For example, as Ca^{2+} accumulates intracellularly, it is known to bind to channels to promote further Ca^{2+} release. We speculate that inclusion of ion channel cooperativity will diminish or remove remaining differences between theoretical expectations and experimental observations.

Galvanovskis and Sandblom, as well as other theoreticians, speculate that intracellular Ca^{2+} oscillations may constitute an appropriate detector with a narrow bandwidth. This, of course, is consistent with our observations of Ca^{2+} oscillations and Ca^{2+} wave in polarized neutrophils. Therefore, certain elements of Galvanovskis and Sandblom's (1997) theoretical treatment are consistent with our experimental observations of weak electric field interactions with living cells.

Signaling promotes MPO surface expression

Although ion channel clustering provides a route to understanding field detection, it does not account for the metabolic changes noted in our previous studies (Kindzelskii and Petty 2000). One bioeffect of Ca^{2+} signaling is the release of intracellular granules. MPO, which is stored within intracellular azurophilic granules, can be secreted by cells (Xu and Hakansson 2002). Furthermore, MPO enhances the amplitudes of metabolic oscillations when it is deposited in the same compartment as the NADPH oxidase (Olsen et al. 2003). Therefore, we tested the ability of phase-matched electric field exposure to affect the disposition of MPO in cells. We found that the electric field treatment protocol resulted in the appearance of MPO at the cell surface. MPO is known to be a highly cationic protein. When MPO was removed from the cell surface or inactivated by inhibitors, the ability of electric fields to influence metabolism was lost. Furthermore, the changes in metabolic oscillations caused by electric field exposure could be mimicked by added purified MPO to untreated neutrophils. We previously suggested cell surface charges played an important role in field detection based upon the finding that neuraminidase treatment, which removes many negative cell surface charges, decreased metabolic amplitude responses to electric field exposure (Kindzelskii and Petty 2000). In the light of our more recent findings presented in this study, it seems likely that the reduction in cell surface charge simply prevented MPO from binding to the cell surface, thereby eliminating the effects of MPO on cell metabolism, as shown here. This model could be further investigated using MPO knock-out mice, which should not display these metabolic responses to phase-matched electric fields, and by using green fluorescent tracers targeted to the azurophilic granules. Signal-mediated MPO trafficking appears to be a likely mechanism of phase-matched electric field effects on neutrophils that accounts for changes in metabolism, oxidant production and DNA damage in response to weak electric fields (Kindzelskii and Petty 2000).

Based upon the experimental observations presented above, we propose a tentative biological model of weak electric field effects on cells (Fig. 20). We believe that electric field exposure simply taps into a pre-existing pathway of neutrophil activation. Polarized cells become responsive because lipid rafts redistribute ion channels into a large cluster or array at the lamellipodium. These cells demonstrate temporal oscillations of Ca^{2+} and NAD(P)H as well as traveling Ca^{2+} and NAD(P)H waves. When a weak electric field is applied to the cells during Ca^{2+} wave propagation, the array of ion channels, whose sensitivity is greatly enhanced by clustering, promote the propagation of a second Ca^{2+} wave, just like receptor stimulation of neutrophils (Kindzelskii and Petty 2003). We speculate that this activation-associated Ca^{2+} wave promotes the release of MPO-containing granules from the cell, which results in MPO accumulation at the cell surface. Neutrophil adherence is sufficient to produce low levels of reactive oxygen metabolite (ROM) production. MPO thereby promotes high amplitude metabolic oscillations (or metabolic resonance) and large amounts of ROM production as described by Olsen et al. (2003). The enhanced levels of ROMs production lead to DNA damage (Kindzelskii and Petty 2000).

Additional implications and corollaries

One corollary suggested by the above data concerns the role of T-type Ca^{2+} channels in neutrophil activation. Recent studies have suggested that mibefradil, originally developed as an anti-hypertensive, has anti-inflammatory properties in animals (Bilici et al. 2001). Although this is presumably mediated by its ability to bind to T-type Ca^{2+} channels, it is not clear which inflammatory cells might be involved or how mibefradil might act as an anti-inflammatory. We now report that T-type channels are expressed by human peripheral blood neutrophils as judged by immunofluorescence microscopy. A previous study from this group has shown that neutrophil activation is accompanied by two traveling Ca^{2+} waves (Kindzelskii and Petty 2003). When the first wave is inhibited, the second wave elicited by the activation stimulus does not form. Consequently, mibefradil's ability to block both Ca^{2+} waves likely explains its ability to act as an anti-inflammatory (Bilici et al. 2001). Various studies indicate that Ca^{2+} signaling plays a central role in

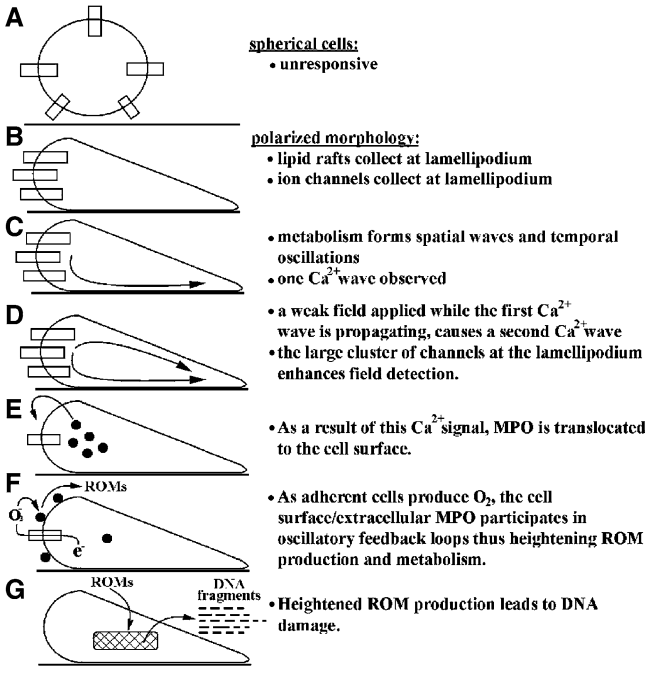

Fig. 20 Summary of how cells detect weak, phase-matched electric fields leading to DNA damage. A schematic model of channel clustering, Ca^{2+} signaling events and MPO trafficking which combine to increase the production of reactive oxygen metabolites (ROM) by neutrophils. Enhanced ROM production leads to DNA damage in the cell. The mechanistic steps are illustrated from *top* to *bottom*

inflammation. Our studies show that T-type Ca^{2+} channels play a central role in these Ca^{2+} signals; we anticipate that several neutrophil functions, such as locomotion and phagolysosome formation, would be reduced by this drug (Kindzelskii and Petty 2003; Worth et al. 2003). Although mibefradil is no longer used as an anti-hypertensive due to dangerous drug interactions, it may be useful in a more limited clinical setting where patients' lives are in immanent danger due to "run-away" inflammatory responses, such as those during septic shock and stage II anthrax. Alternatively, mibefradil-like drugs that do not block the metabolism of other drugs may also be useful in this regard.

The experimental strategy developed to dissect the effects of weak electromagnetic fields on cells has several key advantages. In the analysis of signal transduction pathways, the application of exogenous electric fields has certain advantages. Importantly, the electric field can be applied at the discretion of the observer, without the need to apply ligands or inhibitors to cells. In this way, the signal transduction pathways can be managed by the push of a button. In addition, high speed imaging allows us to spatiotemporally resolve the spatiotemporal dynamics of the Ca^{2+} signaling apparatus. This, in turn, allows us to distinguish between those signaling events unique to responses to electromagnetic fields and those that are associated with other cell signaling phenomena. For example, the counterclockwise Ca^{2+} wave is associated with cellular phenomena such as migration whereas the clockwise Ca^{2+} wave is tied to cell activation responses (Kindzelskii and Petty 2003), including that stimulated by electric fields (this study). This allows us to analyze the multiple channels and signaling waves associated with complex physiological events. In addition, it provides us with a way to study channel function on cells without the necessity of using pharmacological tools.

Our approach to understanding the complex nature of electric field detection by neutrophils provides a paradigm for future studies of weak electric field-to-cell interactions. Our robust analysis of cell-to-field interactions has led to the identification of one type of SKF96365-sensitive membrane channel, likely a SOC of the TRP family of cation channels, as a key participant in the detection of weak phase-matched electric fields. Using molecular biological techniques, such as antisense reagents, it may be possible to identify the channel responsible for ignition of the second Ca^{2+} wave in the presence of an appropriately timed field. Additional characterization of the electric field-sensitive component(s) is currently underway. Furthermore, the identification of SKF96365 as an inhibitor near the electric-field detection mechanism allows other investigators to test the role of SOCs in other bioelectromagnetic experiments.

There has been considerable public concern regarding the health effects of weak electromagnetic fields. Although our data do not speak directly to this point, they do provide a rational mechanism linking channel clusters (this study) with downstream DNA damage (Kindzelskii and Petty 2000). Although time-varying electric fields will not penetrate organisms, time-varying magnetic fields will penetrate tissues. We have shown that brief magnetic field exposure affects neutrophils in vitro (Rosenspire et al. 2003), which suggests the possibility of using time-varying magnetic fields to treat human disease. Instead of focusing on the potentially harmful effects of electromagnetic fields, we believe that more attention should be focused on the potential benefits of using non-invasive time-varying magnetic fields to treat human disease, which may now be possible on the basis of the mechanistic evaluation of signaling reported herein.

Acknowledgements This work was supported by NIH Grant CA74120 (H.R.P.).

References

Aas V, Larsen K, Iverson J (1998) IFN-gamma induces calcium entry in human neutrophils. J Interferon Cytokine Res 18:197–205

Aas V, Larsen K, Iverson LG (1999) Interferon-gamma elicits a G-protein-dependent Ca^{2+} signal in human neutrophils after depletion of intracellular Ca^{2+} stores. Cell Signal 11:101–110

Adachi Y, Kindzelskii AL, Ohno N, Yadomae T, Petty HR (1999) Amplitude and frequency modulation of metabolic signals in leukocytes: synergistic role in interferon-γ and interleukin-6-mediated cell activation. J Immunol 163:4367–4374

Albrecht E, Petty HR (1998) Cellular memory: neutrophil orientation reverses during temporally decreasing chemoattractant concentrations. Proc Natl Acad Sci USA 95:5039–5044

Andreasen D, Jensen BL, Hansen PB, Kwon TH, Nielsen S, Skott O (2000) The alpha(1G)-subunit of a voltage-dependent Ca(2+) channel is localized in rat distal nephron and collecting duct. Am J Physiol Renal Physiol 279:F997–F1005

Bassett CAL (1993) Beneficial effects of electromagnetic fields. J Cell Biochem 51:387–393

Berger W, Prinz H, Striessnig J, Kang H-C, Haugland R, Glossmann H (1994) Complex molecular mechanism for dihydropyridine binding to L-type Ca^{2+} channels as revealed by fluorescence resonance energy transfer. Biochemistry 33:11875–11883

Berton G, Zeni L, Cassatella MA, Rossi F (1986) Gamma interferon is able to enhance the oxidative metabolism of human neutrophils. Biochem Biophys Res Commun 138:1276–1282

Bilici D, Akpinar E, Gursan N, Dengiz GO, Bilici S, Altas S (2001) Protective effect of T-type calcium channel blocker in histamine-induced paw inflammation in rat. Pharmacol Res 44:527–31

Blunck R, Scheel O, Muller M, Brandenburg K, Seitzer U, Seydel U (2001) New insights into endotoxin-induced activation of macrophages: involvement of a K+ channel in transmembrane signaling. J Immunol 166:1009–1015

Bravo-Zehnder M, Orio P, Norambuena A, Wallner M, Meera P, Toro L, Latorre R, Gonzalez A (2000) Apical sorting of a voltage- and Ca2+-activated K+ channel alpha-subunit in Madin-Darby canine kidney cells is independent of N-glycosylation. Proc Natl Acad Sci USA 97:13114–13119

Brazer SC, Singh BB, Liu X, Swaim W, Ambudkar IS (2003) Caveolin-1 contributes to assembly of store-operated Ca^{2+} influx channels by regulating plasma membrane localization of TRPC1. J Biol Chem 278:27208–27215

Brighton CT, Wang W, Seldes R, Zhang G, Pollack SR (2001) Signal transduction in electrically stimulated bone cells. J Bone Joint Surg Am 83A:1514–1523

Cho MR, Thjatte HS, Silvia MT, Golan DE (1999) Transmembrane calcium influx induced by AC electric fields. FASEB J 13:677–683

Davies B, Edwards SW (1989) Inhibition of myeloperoxidase by salicylhydroxamic acid. Biochem J 258:801–806

Ding AH, Nathan CF, Stuehr DJ (1988) Release of reactive nitrogen intermediates and reactive oxygen intermediates from mouse peritoneal macrophages. J Immunol 141:2407–2412

Duke TAJ, Bray D (1999) Heightened sensitivity of a lattice of membrane receptors. Proc Natl Acad Sci USA 96:10104–10108

Dykstra M, Cherukuri A, Sohn HW, Tzeng SJ, Pierce SK (2003) Location is everything: lipid rafts and immune cell signaling. Annu Rev Immunol 21:457–481

Eichwald C, Kaiser F (1993) Model for receptor-controlled cytosolic calcium oscillations and for external influences on the signal pathway. Biophys J 65:2047–2058

Eichwald C, Kaiser F (1995) Model for external influences on cellular signal transduction pathways including cytosolic calcium oscillations. Bioelectromagnetics 16:75–85

Fang KS, Farboud B, Nuccitelli R, Isseroff RR (1998) Migration of human keratinocytes in electric fields requires growth factors and extracellular calcium. J Invest Dermatol 111:571–576

Franke K, Gruler H (1994) Directed cell movement in pulsed electric fields. Z Naturforsch 49c:241–249

Galvanovskis J, Sandblom J (1997) Amplification of electromagnetic signals by ion channels. Biophys J 73:3056–3065

Gamberucci A, Giurisato E, Pizzo P, Tassi M, Giunti R, McIntosh DP, Benedetti A (2000) Diacylglycerol activates the influx of extracellular cations in T-lymphocytes independently of intracellular calcium-store depletion and possibly involving endogenous TRP6 gene products. Biochem J 364:245–254

Goligorsky MS, Colflesh D, Gordienko D, Moore LC (1995) Branching points of renal resistance arteries are enriched L-type calcium channels and initiate vasoconstriction. Am J Physiol 268:F251–F257

Haga Y, Dumitrescu A, Zhang Y, Stain-Malmgren R, Sjoquist PO (1996) Effects of calcium blockers on the cytosolic calcium, H_2O_2 production and elastase release in human neutrophils. Pharmacol Toxicol 79:312–317

Halaszovich CR, Zitt C, Jungling E, Luckhoff A (2000) Inhibition of TRP3 channels by lanthanides. Block from the cytosolic side of the plasma membrane. J Biol Chem 275:37423–37428

Hayat S, Wigley CB, Robbins J (2003) Intracellular calcium handling in rat olfactory ensheathing cells and its role in axonal regeneration. Mol Cell Neurosci 22:259–270

Heiner I, Eisfeld J, Halaszovich CR, Wehage E, Jungling E, Zitt C, Luckhoff A (2003) Expression profile of the transient receptor potential (TRP) family in neutrophil granulocytes: evidence for currents through long TRP channel 2 induced by ADP-ribose and NAD. Biochem J 371:1045–1053

Hill WG, An B, Johnson JP (2002) Endogenously expressed epithelial sodium channel is present in lipid rafts in A6 cells. J Biol Chem 277:33541–33544

Hoppe W, Lohmann W, Markl H, Ziegler H (1983) Biophysics. Springer, Berlin Heidelberg New York

Hotary KB, Robinson KR (1994) Endongenous electrical currents and voltage gradients in Xenopus embryos and the consequences of their disruption. Dev Biol 166:789–800

Irita K, Fujita I, Takeshige K, Minakami S, Yoshitake J (1986) Calcium channel antagonist induced inhibition of superoxide production in human neutrophils. Mechanisms independent of antagonizing calcium influx. Biochem Pharmacol 35:3465–3471

Itagakin K, Kannan KB, Livingston DH, Deitch EA, Fekete Z, Hauser CJ (2002) Store-operated calcium entry in human neutrophils reflects multiple contributions from independently regulated pathways. J Immunol 168:4063–4069

Jaffe LF, Nuccitelli R (1977) Electrical controls of development. Annu Rev Biophys Bioeng 6:445–476

Jager U, Gruler H, Bultmann B (1988) Morphological changes and membrane potential of human granulocytes under influence of chemotactic peptide and/or echo-virus, type 9. Klin Wochenschr 66:434–436

Jerlich A, Fritz G, Kharrazi H, Hammel M, Tschabuschnig S, Glatter O, Schaur RJ (2000) Comparison of HOCl traps with myeloperoxidase inhibitors in prevention of low density lipoprotein oxidation. Biochim Biophys Acta 1481:109–118

Kenny JS, Kisaalita WS, Rowland G, Thai C, Foutz T (1997) Quantitative study of calcium uptake by tumorigenic bone (TE-85) and neuroblastoma *x* glioma (NG108–15) cells exposed to extremely-low-frequency (ELF) electric fields. FEBS Lett 414:343–348

Kindzelskii AL, Petty HR (2000) Extremely low frequency electric fields promote neutrophil extension, metabolic resonance and DNA damage during migration. Biochim Biophys Acta 1495:90–111

Kindzelskii AL, Petty HR (2002) Apparent role of traveling metabolic waves in periodic oxidant release by living cells. Proc Natl Acad Sci USA 99:9207–9212

Kindzelskii AL, Petty HR (2003) Intracellular calcium waves accompany neutrophil polarization, formylmethionylleucylphenylalanine stimulation, and phagocytosis: a high speed microscopy study. J Immunol 170:64–72

Kindzelskii AL, Laska ZO, Todd RF III, Petty HR (1996) Urokinase-type plasminogen activator receptor reversibly dissociates from complement receptor type 3 ($\alpha_M\beta_2$) during neutrophil polarization. J Immunol 156:297–309

Kindzelskii AL, Eszes MM, Todd RF III, Petty HR (1997) Proximity oscillations of complement receptor type 4 and urokinase receptors on migrating neutrophils are linked with signal transduction/metabolic oscillations. Biophys J 73:1777–1784

Kindzelskii AL, Yang Z, Nabel GJ, Todd RF III, Petty HR (2000) Ebola virus secretory glycoprotein (sGP) disrupts FcγRIIIB to CR3 proximity on neutrophils. J Immunol 164:953–958

Knaus HG, Moshammer T, Friedrich K, Kang HG, Haugland RP, Glossmann H (1992) In vivo labeling of L-type Ca^{2+} channels by fluorescent dihydropyridines: evidence for a functional,

extracellular heparin-binding site. Proc Natl Acad Sci USA 89:3586–3590
Knaus HG, Moshammer T, Kang HG, Haugland RP, Glossmann H (1992) A unique fluorescent phenylakylamine probe for L-type Ca^{2+} channels. J Biol Chem 267:2179–2189
Koo GC, Blake JT, Talento A, Nguyen M, Lin S, Sirotina A, Shah K, Mulvany K, Hora Jr D, Cunningham P, Wunderler DL, McManus OB, Slaughter R, Bugianesi R, Felix J, Garcia M, Williamson J, Kaczorowski G, Sigal NH, Springer MS, Feeney W (1997) Blockade of the voltage-gated potassium channel Kv1.3 inhibits immune responses in vivo. J Immunol 158:5120–5128
Leonard RJ, Garcia ML, Slaughter RS, Reuben JP (1992) Selective blockers of voltage-gated K+ channels depolarize human T lymphocytes: mechanism of the antiproliferative effect of charybdotoxin. Proc Natl Acad Sci USA 89:10094–10098
Lewis RS, Cahalan MD (1995) Potassium and calcium channels in lymphocytes. Annu Rev Immunol 13:623–653
Lin CS, Boltz RC, Blade JT, Nguyen M, Talento A, Fischer PA, Springer MS, Sigal NH, Slaughter RS, Garcia ML (1993) Voltage-gated potassium channels regulate calcium-dependent pathways involved in human T lymphocyte activation. J Exp Med 177:637–645
Lindstrom E, Lindstrom P, Berglund A, Lundgren E, Mild KH (1995) Intracellular calcium oscillations in a T-cell line after exposure to extremely low-frequency magnetic fields with variable frequencies and flux densities. Bioelectromagnetics 16:41–47
Lockwich TP, Liu X, Singh BB, Jadlowiec J, Weiland S, Ambudkar IS (2000) Assembly of Trp1 in a signaling complex associated with caveolin-scaffolding lipid raft domains. J Biol Chem 275:11934–11942
Lorich DG, Brighton CT, Gupta R, Corsetti JR, Levine SE, Gelb IB, Seldes R, Pollack SR (1998) Biochemical pathway mediating the response of bone cells to capacitive coupling. Clin Orthop 350:246–256
Luscinskas FW, Mark DE, Brunkhorst B, Lionetti FJ, Cragoe EJ Jr, Simons ER (1988) The role of transmembrane cationic gradients in immune complex stimulation of human polymorphonuclear leukocytes. J Cell Physiol 134:211–219
Lyle DB, Ayotte RD, Sheppard AR, Adey WR (1988) Suppression of T-lymphocyte cytotoxicity following exposure to 60-Hz sinusoidal electric fields. Bioelectromagnet 9:303–313
Lyle DB, Wang X, Ayotte RD, Sheppard AR, Adey WR (1991) Calcium uptake by leukemic and normal T-lymphocytes exposed to low frequency magnetic fields. Bioelectromagnetics 12:145–156
Majander A, Wikstrom M (1989) The plasma membrane potential of human neutrophils. Role of ion channels and the sodium/potassium pump. Biochim Biophys Acta 980:139–145
Manes S, Mira E, Gomez-Mouton C, Lacalle RA, Keller P, Labrador JP, Martinez-A C (1999) Membrane raft microdomains mediate front-rear polarity in migrating cells. EMBO J 18:6211–6220
Marks PW, Maxfield FR (1990) Transient increases in cytosolic free calcium appear to be required for the migration of adherent human neutrophils. J Cell Biol 110:43–52
Martens JR, Sakamoto N, Sullivan SA, Grobaski TD, Tamkun MM (2001) Isoform-specific localization of voltage-gated K+ channels to distinct lipid raft populations. Targeting of Kv1.5 to caveolae. J Biol Chem 276:8409–8414
Maxfield FR, Kruskal BA (1987) Cytosolic free calcium increases before and oscillates during frustrated phagocytosis in macrophages. J Cell Biol 105:2685–2693
Minke B, Cook B (2002) TRP channel proteins and signal transduction. Physiol Rev 82:429–472
Mori Y, Wakamori T, Miyakawa T, Hermosura M, Hara Y, Nishida M, Hirose K, Mizushima A, Kurosaki M, Mori E, Gotoh K, Okada T, Fleig A, Penner R, Iino M, Kurosaki T (2002) Transient receptor potential 1 regulates capacitative Ca(2+) entry and Ca(2+) release from endoplasmic reticulum in B lymphocytes. J Exp Med 195:673–681
Nachman-Clewner M, St Jules R, Townes-Anderson E (1999) L-type calcium channels in the photoreceptor ribbon synapse: localization and role in plasticity. J Comp Neurol 415:1–16
Neumann E (2000) Digression on chemical electromagnetic field effects in membrane signal transduction—cooperativity paradigm of the acetylcholine receptor. Bioelectrochemistry 52:43–49
Nishimura KY, Isseroff RR, Nuccitelli R (1996) Human keratinocytes migrate towards the negative pole in direct current electric fields comparable to those measured in mammalian wounds. J Cell Sci 109:199–207
Nuccitelli R (1988) Physiological electric fields can influence cell motility, growth and polarity. Adv Cell Biol 2:213–233
Olsen LF, Kummer U, Kindzelskii AL, Petty HR (2003) A model of the oscillatory metabolism of activated neutrophils. Biophys J 84:69–81
Onuma EK, Hui SW (1988) Electric field-directed cell shape changes, displacement, and cytoskeletal reorganization are calcium dependent. J Cell Biol 106:2067–2075
Oshima T, Ikeda K, Furukawa M, Ueda N, Suzuki H, Takasaka T (1996) Distribution of Ca^{2+} channels on cochlear outer hair cells revealed by fluorescent dihydropyridines. Amer J Physiol 271:C944–C949
Perez-Reyes E (2003) Molecular physiology of low-voltage-activated T-type calcium channels. Physiol Rev 83:117–161
Perret S, Cantereau A, Audin J, Dufy B, Georgescauld D (1999) Interplay between Ca^{2+} influx underlies localized hyperpolarization-induced [Ca^{2+}]i waves in prostatic cells. Cell Calcium 25:297–311
Petty HR (1993) Molecular biology of membranes. Plenum Press, New York
Petty HR (2000) Oscillatory signals in migrating neutrophils: Effects of time-varying chemical and electrical fields. In: Walleczek J (ed) Self-organized biological dynamics and nonlinear control by external stimuli. Cambridge University Press, Cambridge, pp 173–192
Petty HR (2001) Neutrophil oscillations: temporal and spatiotemporal aspects of cell behavior. Immunol Res 23:125–134
Petty HR, Kindzelskii AL (2000) Dissipative metabolic structures in living cells: observation of target patterns during cell adherence. J Phys Chem B 104:10952–10955
Petty HR, Worth RG, Kindzelskii AL (2000) Imaging sustained dissipative patterns in the metabolism of individual living cells. Phys Rev Lett 84:2754–2757
Pike LJ (2003) Lipid rafts: bringing order to chaos. J Lipid Res 44:655–667
Pizzo P, Burgo A, Pozzan T, Fasolato C (2001) Role of capacitative calcium entry on glutamate-induced calcium influx in type-I rat cortical astrocytes. J Neurochem 79:98–109
Rauer H, Grissmer S (1999) The effect of deep pore mutation on the action of phenylalkylamines on the Kv1.3 potassium channel. Br J Pharmacol 127:1065–1074
Robe RJ, Grissmer S (2000) Block of the lymphocyte K^+ channel mKv1.3 by the phenylalkylamine verapamil: kinetic aspects of block and disruption of accumulation of block by a single point mutation. Br J Pharmacol 131:1275–1284
Rosenspire AJ, Kindzelskii AL, Petty HR (2000) Interferon-γ and sinusoidal electric fields signal by modulating NAD(P)H oscillations in polarized neutrophils. Biophys J 79:3001–3008
Rosenspire AJ, Kindzelskii AL, Petty HR (2001) Pulsed DC electric fields couple to natural NAD(P)H oscillations in HT1080 fibrosarcoma cells. J Cell Sci 114:1515–1526
Rosenspire AJ, Kindzelskii AL, Simon BJ, HR Petty (2003) Real time control of neutrophil metabolism by very weak ELF magnetic fields. Bioelectromagnetics Society Abstract Book 25:33
Rothberg BS (2004) Allosteric modulation of ion channels: the case of maxi-K. Sci STKE (http://www.stke.org/cgi/content/full/sigtrans;2004/227/pe16)
Sadighi Akha AA, Willmott NJ, Brickley K, Dolphin AC, Galione A, Hunt SV (1996) Anti-Ig-induced calcium influx in rat B lymphocytes mediated by cGMP through a dihydropyridine-sensitive channel. J Biol Chem 271:7297–7300

Schienbein M, Gruler H (1995) Chemical amplifier, self-ignition, and amoeboid cell migration. Phys Rev E 52:4183–4197

Schild D, Geiling H, Bischofberger J (1995) Imaging of L-type Ca^{2+} channels in olfactory bulb neurons using fluorescent dihydropyridine and a styryl dye. J Neurosci Methods 59:183–190

Sehgal G, Zhang K, Todd RF, Boxer LA, Petty HR (1993) Lectin-like inhibition of immune complex receptor-mediated stimulation of neutrophils. Effects on cytosolic calcium release and superoxide production. J Immunol 150:4571–4580

Shaw SL, Quatrano RS (1990) Polar localization of a dihydropyridine receptor on living Fucus zygotes. J Cell Sci 109:335–342

Sheridan DM, Isseroff RR, Nuccitelli R (1996) Imposition of a physiologic DC electric field alters the migratory response of human keratinocytes on extracellular matrix molecules. J Invest Dermatol 106:642–646

Shi R, Borgens RB (1995) Three-dimensional gradients of voltage during development of the nervous system's invisible coordinates for the establishment of embryonic pattern. Dev Dyn 202:101–114

Silvius JR (2003) Role of cholesterol in lipid raft formation: lessons from lipid model systems. Biochim Biophys Acta 1610:174–183

Simchowitz L, Spilberg I (1979) Generation of superoxide radicals by human peripheral neutrophils activated by chemotactic factor. Evidence for the role of calcium. J Lab Clin Med 93:583–593

Sitrin RG, Pan PM, Blackwood RA, Huang J-B, Petty HR (2001) Evidence for a signaling partnership between urokinase receptors (CD87) and L-selectin (CD62L) in human polymorphonuclear neutrophils. J Immunol 166:4822–4825

Sitrin RG, Johnson DR, Pan PM, Harsh DM, Huang J, Petty HR, Blackwood RA (2004) Lipid raft compartmentalization of urokinase receptor signaling in human neutrophils. Am J Respir Cell Mol Biol 30:233–241

Stewart R, Erskine L, McCaig CD (1995) Calcium channel subtypes and intracellular calcium stores modulate electric field-stimulated and–oriented nerve growth. Dev Biol 171:340–351

Trevino CL, Serrano CJ, Beltran C, Felix R, Darszon A (2001) Identification of mouse trp homologs and lipid rafts from spermatogenic cells and sperm. FEBS Lett 509:119–125

Trollinger DR, Isseroff RR, Nuccitelli R (2002) Calcium channel blockers inhibit galvanotaxis in human keratinocytes. J Cell Physiol 193:1–9

Uckum FM, Kurosaki T, Jin J, Jun X, Morgan A, Takata M, Bolen J, Luben R (1995) Exposure of B-lineage lymphoid cells to low energy electromagnetic fields stimulates Lyn kinase. J Biol Chem 270:27666–27670

Vallee N, Briere C, Petitprez M, Barthou H, Souvre A, Alibert G (1997) Studies on ion channel antagonist-binding sites in sunflower protoplasts. FEBS Lett 411:115–118

Vazquez G, Lievremont JP, St J Bird G, Putney JW Jr (2001) Human Trp3 forms both inositol trisphosphate receptor-dependent and receptor-independent store-operated cation channels in DT40 avian B lymphocytes. Proc Natl Acad Sci USA 98:11777–11782

Visegrady A, Lakos Z, Czimbalek L, Somogyi B (2001) Stimulus-dependent control of inositol 1,4,5-trisphosphate-induced Ca(2+) oscillation frequency by the endoplasmic reticulum Ca(2+)-ATPase. Biophys J 81:1398–1405

Walleczek J, Liburdy RP (1990) Nonthermal 60 Hz sinusoidal magnetic field exposure enhances $_{45}Ca^{2+}$ uptake in rat thymocytes: dependence on mitogen activation. FEBS Lett 271:157–160

Wang E, Zhao M, Forrester JV, McCaig CD (2000) Re-orientation and faster, directed migration of lens epithelial cells in a physiological electric field. Exp Eye Res 71:91–98

Weiergraber M, Pereverzev A, Vajna R, Henry M, Schramm M, Nastainczyk W, Grabsch H, Schneider T (2000) Immunodetection of alpha1E voltage-gated Ca(2+) channel in chromogranin-positive muscle cells of rat heart, and in distal tubules of human kidney. J Histochem Cytochem 48:807–819

Willmott NJ, Choudhury Q, Flower RJ (1996) Functional importance of the dihydropyridine-sensitive, yet voltage-insensitive store-operated Ca2+ influx of U937 cells. FEBS Lett 394:159–164

Witkowski FX, Leon LJ, Penkoske PA, Giles WR, Spano ML, Ditto WL, Winfree AT (1998) Spatiotemporal evolution of ventricular fibrillation. Nature 392:78–82

Worth RG, Kim M-K, Kindzelskii AL, Petty HR, Schreiber AD (2003) Signal sequence within FcγRIIA controls calcium wave propagation patterns: apparent role in phagolysosome fusion. Proc Natl Acad Sci USA 100:4533–4538

Xu X, Hakansson L (2002) Degranulation of primary and secondary granules in adherent human neutrophils. Scand J Immunol 55:178–188

Yost MG, Liburdy RP (1992) Time-varying and static magnetic fields act in combination to alter calcium signal transduction in lymphocytes. FEBS Lett 296:117–122

Zarewych DM, Kindzelskii AL, Todd III RF, Petty HR (1996) Lipopolysaccharide induces CD14 association with complement receptor type 3 which is reversed by neutrophil adhesion. J Immunol 156:430–433

Zhuang H, Wang W, Seldes RM, Tahernia AD, Fan H, Brighton CT (1997) Electrical stimulation induces the level of TGF-beta 1 mRNA in osteoblastic cells by a mechanism involving calcium/calmodulin pathway. Biochem Biophys Res Commun 237:225–229